Coming to Grips with N−H···N Bonds. 1. Distance Relationships and Electron Density at the Bond Critical Point

Osvald Knop,* Kathryn N. Rankin, and Russell J. Boyd†

Department of Chemistry, Dalhousie University, Halifax NS, Canada B3H 4J3

Received: February 17, 2001; In Final Form: May 3, 2001

In an attempt to discover and analyze trends in distance relationships and properties at the bond critical point (BCP) in linear or near-linear N−H···N hydrogen bonds, the geometry of such bonds in a large number of suitable simple chemical species was optimized at the RHF/6-31G** level. The results for 67 of these are reported here; the geometry of 19 of them was optimized also at the MP2/6-31G** level. Correlations between the internuclear N−H, H···N, and N···N separations as well as between the N···BCP and H···BCP distances for these data sets and for different model functions are described in detail. The special case of symmetric N−H−N bonds is discussed; comparison with available experimental evidence shows that the correlation functions derived from the ab initio data have useful predictive value for crystallographic determinations involving short N−H−N bonds. Analysis of the correlation between the d(N−H) distance and the electron density ρ_c at the BCP has shown that although acceptable d,ρ_c representations are obtained when ρ_c is fitted over the entire d(N−H) range by a single model function, significantly better fits result for both the 6-31G** and the MP2/6-31G** set when *two* separate regression functions of the same type are used, one for the covalent and another for the H···N bonds. The implications of these findings are discussed. The results of the correlation analysis of the curvatures λ_i, the Laplacians $\nabla^2\rho_c$, and the kinetic energy densities at the BCP, based on the data presented in this paper, will be reported in a subsequent paper, together with some aspects of the energy of formation of the N−H···N bonds.

Prefatory Note

The RHF/6-31G** geometry optimization used in most of the calculations in this paper was adopted mainly to generate, within the intended scope of this exploratory study, a homogeneous body of results that would be sufficiently large to reveal and describe the existence of such consistent trends in the properties of N−H−N bonds as may be evident in this model. This optimization was manageable at the practical level, and it rendered equilibrium N−H−N geometries that are comparable to experiment. It is expected that the analysis and conclusions presented here will provide a basis for further exploration and verification, at a more elaborate theory level and by experiment, of the trends we report. The present paper is concerned with those properties in Tables 1−4 that relate to the geometry of, and the electron density at the bond critical points in, the N−H−N bonds investigated. The remaining data in Tables 1−4 will be analyzed for correlations in a subsequent paper, now in preparation.

Notation

In a complete N_d−H···N_a hydrogen bond, N_d is the donor and N_a the acceptor atom. Unprimed quantities (e.g., the internuclear distance d, the electron density ρ_c at the bond critical point BCP, the Laplacian $\nabla^2\rho_c$) refer indiscriminately to the covalent N_d−H and the H-bond H···N_a components of the bond. Primed entities (e.g., d', the bond critical point X′) refer to the N_d−H component and the doubly primed entities (e.g., d'', X″) to the H···N_a component. Other symbols are defined in Tables 1 and 2 and as they are encountered in the text for the first time. Numerical values of the quantities discussed are given in atomic units (au) except for the distances, which are given in Å for convenience of comparison with experimental values. Throughout, HF will refer to complete RHF/6-31G** geometry optimizations unless stated otherwise. Together, the species listed in Table 1 constitute the sample **S**.

Introduction

Although considerably less attention has been lavished on an understanding of the properties of N−H−N hydrogen bonds than on their oxygen-involving heteronuclear counterparts,[1] the N−H−N bonds do not lack in importance and interest, not least because of their potential involvement in biological systems. Steiner[2] surveyed the geometry of 31 N−H−N bonds (1.6 Å < d'' < 2.4 Å) in which the H atom had been located by high-quality neutron diffraction. He found a high degree of correlation between the d' and d'' internuclear distances. This he was able successfully to represent by the function

$$d' = d_0 - b \ln\{1 - \exp[(d_0 - d'')/b]\} \qquad (1)$$

which is based on an adaptation of Pauling's bond order equation[3], $D(n) = D(1) - B \ln n$, to conjugate bond lengths in 3c4e bonds: $d'(s') = d_0 - b \ln s'$, $d''(s'') = d_0 - b \ln s''$, $s' + s'' = 1$ (s', s'' = bond orders, d_0 = limiting N−H bond length).[4] The function is symmetric about the $d' = d''$ line, i.e., d' and d'' are interchangeable. In a *symmetric* N−H−N bond, $d' = d'' = d_{sym} = d_0 + b \ln 2$. For Steiner's sample, the regression

* To whom correspondence should be addressed. Fax: (902) 494-1310.
† E-mail: russell.boyd@dal.ca.

10.1021/jp0106348 CCC: $20.00
Published on Web 06/12/2001

coefficients were

$$d_0 = 0.996 \text{ Å}, b = 0.381 \text{ Å} \quad (2)$$

yielding $d_{sym} = 1.260$ Å. This value is in agreement with the d_{sym} distance reported[5] for the shortest known, linear symmetric N−H−N bond, that in the inside-protonated (intrabridgehead) cation of 1,6-diazabicyclo[4.4.4]tetradecane (henceforth referred to as $[4.4.4]^+$). The N···N distance in the chloride of this cation (X-ray diffraction at room temperature) is quoted as 2.526(3) Å; the centrosymmetric (single-well) geometry of this bond has been deduced from the X-ray crystallographic D_3 symmetry of the cation and the thermal parameters of the H atom, from neutron diffraction[6,7] at 20 K (not included in Steiner's sample),[8] and from NMR and IR spectra.[9] The $d_{sym} = 1.26$ Å is also compatible with the ab initio estimates obtained by Scheiner[10] from his analysis of the requirements for the existence of symmetric N−H−N bonds.

For linear or near-linear N−H···N bonds, (1) can be reformulated to include the N···N distance $D = d' + d''$:

$$D = d_0 + d'' - b \ln\{1 - \exp[(d_0 - d'')/b]\} = d_0 + d' - b \ln\{1 - \exp[(d_0 - d')/b]\} \quad (3)$$

This form is particularly useful in that it permits estimates of the position of the H atom in such bonds from the positions of the two N atoms, which in structures determined from X-ray data are more accurately known than the position of the H atom (see, for example, ref 11).

The rapidly expanding activity and interest (including our own[12]) in experimental determinations of charge densities and bond critical parameters (the electron density ρ_c and the Laplacian $\nabla^2(\rho_c)$ at the BCP, etc.) of hydrogen bonds[13] have prompted us to look for an account of the properties of N−H···N bonds that would combine bond geometry with these bond critical parameters and result in a predictive scheme. Basing such an account on the experimental results available to date has its difficulties. In Steiner's sample, the shortest bonds have d'' not below 1.6 Å, and with the exception of $[4.4.4]^+$, even in the bonds reported as symmetric the d'' is not below ∼1.3 Å (see below). We do not know whether this gap in the N−H···N geometry exists because of an as yet insufficient experimental effort (preparability, crystallography, MW spectroscopy) or for other reasons, possibly intrinsic. Second, bond critical parameters determined by experiment have so far been reported for only a few N−H···N bonds. In some of them, the H atom has not been located by matching neutron diffraction, and the haphazard accumulation of experimental determinations does not ensure a uniform distribution of N−H···N geometries over the d range. Under these circumstances, recourse to a reasonably extensive, systematic ab initio study seemed to be the most promising approach to elucidating properties of N−H···N bonds as a class. This paper is an account of such a goal-oriented exploratory investigation.

Effort was made for the sample **S** (Table 1) to be representative, both as to geometry and chemical variety, over as wide a d range as possible. This explains the inclusion in **S** of a number of exotic and hypothetical molecular species, some of which may be inaccessible to experiment, being incapable, under laboratory conditions, of independent existence vis-à-vis more stable competing species or systems. The well-tested and documented RHF/6-31G** scheme was employed to generate optimized molecular geometries and bond critical parameters sufficiently realistic to reveal underlying trends and sufficiently accurate for such trends to be evaluated analytically or statistically. This scheme was used throughout except for occasional MP2/6-3lG** level verification checks, as described.

The optimizations were performed using GAUSSIAN94[14] and supplemented using the AIMPAC[15] program package. The results listed in Tables 1 and 2 are those for point-group symmetries that yielded the lowest total electronic energies E. The highest geometrically possible symmetry was assumed for the initial geometry and the result was compared to subsequent optimizations in one or more subgroup symmetries, as required (cf. Table 1). For a few of the species (**17**, **59**, **64**, **65**), acceptable optimization was not achieved in any of the symmetries tried (one or more imaginary frequencies, gross discrepancies in parameter correlations). However, these species subsequently were successfully optimized in MP2/6-31G**, which confirmed their ab initio existence as H-bonded species. The results of the MP2 optimizations are collected in Tables 3 and 4.

Details of the optimized equilibrium molecular geometries (Cartesian coordinates of the atoms, bond lengths and angles other than those in the N−H−N bonds, etc.) were thought too voluminous even for the Supporting Information. However, structural and other features of particular interest will be extracted for separate publication elsewhere.

Distance Relationships

Relationships between *d′*, *d″*, and *D*. The d', d'' pairs in **S** extend the d'' range of Steiner's sample (Figure lA). Like those of the Steiner set, they are all well fitted by (1) as the model function. The regression of d' on d'' yields

$$d_0 = 0.981(3) \text{ Å}, b = 0.386\ (9) \text{ Å}, d_{sym} = 1.249(9) \text{ Å}, D_{min} = 2.497(19) \text{ Å} \quad (4)$$

($r^2 = 0.896$, $\sigma = 0.011$ Å); the regression coefficients d_0 and b are strongly correlated, $r = -0.93$). The residuals are distributed quite uniformly. The scatter in Figure lA may thus be attributed to the natural variation in **S**.

Although the regression coefficients (4) are similar to those of Steiner's regression (2) for the experimental data set, statistical tests on the sums of squares of the residuals show that representing the **S** data by (1) + (2) can be strongly rejected in favor of the independently fitted (1) + (4) function. The difference between Steiner's d' [(1) + (2)] function, for the experimental data set, and our d' [(l) + (4)], for the HF set, is everywhere positive. It increases with decreasing d'' up to ∼0.017 Å at the short end of our d'' range and is ∼0.023 Å at d_{sym}; with increasing d'' it tends to a residual asymptotic value of ∼0.015 Å. The optimized d', d'' distances are thus consistently undervalued relative to experiment (at finite temperatures), in agreement with the general expectation for 6-31G**-optimized internuclear distances. To this extent, the optimized d', d'' are validated by experiment to a remarkably high degree over the entire d'' range examined. The difference between Steiner's $d_{sym} = 1.260$ Å and that from (1) + (4) is 0.012 Å (0.017 Å if taken along the 45° symmetry line of the plot), i.e., within 2σ of d_{sym} from (4).

It is to be noted that while the d'' values of Table 2 extend quite far, to ∼2.5 Å and in a coherent sequence of optimized geometries, the *smallest* d'' (in **1**) is still ∼0.22 Å away from the d_{sym} estimated from the regression. This is elaborated upon below.

The internuclear distance relationships can be presented in other instructive ways. For *linear* N−H···N bonds the means of the conjugate d', d'' pairs, when plotted against D (Figure 2A), would fall by definition on a rectilinear locus $(d' + d'')/2$

TABLE 1: RHF/6-31G Optimized Equilibrium Molecular Geometries**[a]

configuration[b]	PG[c]	N_dHN_a[d] (deg)	$-E$	$-E_f$[e]	$\epsilon(N_d)$	ϵ(H)	$\epsilon(N_a)$	other PGs tried[f]
1 $[F_3NH\cdots NCF]^+$	C_{3v}	(180)	544.51968	0.05101	0.846	0.558	−0.502	C_1
2 $[FCNH\cdots NCF]^+$	$C_{\infty v}$	(180)	383.71465	0.04022	−0.389	0.559	−0.472	$[C_s]$, C_1
3 $[HCNH\cdots NCH]^+$	$C_{\infty v}$	(180)	186.08449	0.04205	−0.417	0.546	−0.488	$[D_{\infty h}]$, C_s
4 $[LiCNH\cdots NCLi]^+$	$C_{\infty v}$	(180)	199.97935	0.05528	−0.482	0.511	−0.545	C_s
5 $[OCNH\cdots NCO]^-$	C_s	179.6	335.00171	0.04025	−0.669	0.473	−0.736	$[D_{\infty h}]$, $[C_{\infty v}]$, $[C_{2h}]$, $[C_{2v}]$
6 $[HCNH\cdots NCF]^+$	$C_{\infty v}$	(180)	284.90120	0.03863	−0.411	0.539	−0.471	C_s
7 $[SCNH\cdots NCS]^-$	$C_{\infty v}$	(180)	980.31416	0.04569	−0.537	0.482	−0.603	$[D_{\infty h}]$, C_s
8 $[FH_2NH\cdots NH_3]^+$	C_s	174.6	211.52114	0.05078	−0.189	0.494	−0.878	
9 $[F_3NH\cdots NCCN]^+$	C_{3v}	(180)	537.39817	0.03555	0.870	0.534	−0.584	C_1
10 $[NCCNH\cdots NCCN]^+$	$C_{\infty v}$	(180)	369.47087	0.02843	−0.491	0.534	−0.550	$[D_{\infty h}]$, C_s, C_1
11 $[CNH\cdots NC]^-$	$C_{\infty v}$	(180)	185.19336	0.04799	−0.510	0.465	−0.616	$[D_{\infty h}]$, C_s
12 $[H_3NH\cdots NCS\cdots HNH_3]^+$	C_s	176.4	603.19418	0.22919	−0.718	0.482	−0.606	
13 $[CNH\cdots NCO]^-$	$C_{\infty v}$	(180)	260.10042	0.04864	−0.504	0.466	−0.739	C_s
14 $[H_3NH\cdots NCLi]^+$	C_{3v}	(180)	156.38789	0.06986	−0.718	0.474	−0.574	C_s, C_1
15 $[FCNH\cdots NCCN]^+$	$C_{\infty v}$	(180)	376.59529	0.02691	−0.373	0.531	−0.542	C_1
16 $[HCNH\cdots NCCN]^+$	$C_{\infty v}$	(180)	277.78232	0.02580	−0.401	0.517	−0.537	C_s
17 $[CNH\cdots NNN]^-$	C_s	176.8	256.16140	0.04068	−0.501	0.449	−0.710	$[C_{\infty v}]$, $[C_1]$
18 $[OCNH\cdots NNN]^-$	C_1	175.8	331.06322	0.03610	−0.701	0.452	−0.711	$[C_s]$
19 $[F_2HNH\cdots NCCN]^+$	C_s	178.3	438.63903	0.02853	0.390	0.489	−0.559	
20[f] $[FH_2NH\cdots NH_2F]^+$	C_s	144.1	310.27404	0.03631	−0.112	0.444	−0.307	
21 $[H_3NH\cdots NH_3]^+$	C_{3v}	(180)	112.78284	0.04177	−0.712	0.459	−0.878	$[D_{3d}]$, C_s, C_1
22 $[CNH\cdots NCS]^-$	$C_{\infty v}$	(180)	582.76701	0.03507	−0.498	0.444	−0.591	C_s
23 $[F_2HNH\cdots NHF_2]^+$	C_s	172.4	507.78940	0.03137	0.392	0.490	0.212	
24 $[LiCNH\cdots NH_2F]^+$	C_1	172.5	255.13858	0.02408	−0.481	0.474	−0.310	
25 $[OCNH\cdots NCS]^-$	C_s	177.4	657.66839	0.02843	−0.833	0.543	−0.819	$[C_{\infty v}]$
26 $SCNH\cdots NCLi$	C_s	179.9	590.19244	0.02380	−0.558	0.431	−0.491	
27 $[LiCNH\cdots NCH]^+$	C_s	174.7	193.05438	0.02567	−0.470	0.462	−0.455	$[C_{\infty v}]$, $[C_1]$
28 $SCNH\cdots NH_3$	C_{3v}	(180)	546.61156	0.01987	−0.588	0.438	−0.843	C_s
29 $[LiCNH\cdots NCF]^+$	$C_{\infty v}$	(180)	291.87255	0.02371	−0.471	0.462	−0.443	C_s
30 $[NNNH\cdots NNN]^-$	C_s	179.5	327.13346	0.02946	−0.559	0.410	−0.701	$[D_{\infty h}]$, $[C_{\infty v}]$, $[C_{2h}]$, $[C_{2v}]$
31 $[FH_2NH\cdots NCCN]^+$	C_s	179.6	339.88937	0.02335	−0.133	0.463	−0.539	
32 $[F_3NH\cdots NF_3]^+$	C_{3v}	(180)	705.32217	0.01071	0.909	0.485	0.756	C_1
33 $[H_3NH\cdots NCH]^+$	C_{3v}	(180)	149.45569	0.03302	−0.692	0.450	−0.488	C_s
34 $[H_3NH\cdots NCF]^+$	C_{3v}	(180)	248.27300	0.03020	−0.692	0.451	−0.478	C_s
35 $CNH\cdots NCLi$	$C_{\infty v}$	(180)	192.65165	0.01954	−0.507	0.416	−0.483	C_s
36 $CNH\cdots NH_3$	C_{3v}	(180)	149.07218	0.01702	−0.525	0.424	−0.834	C_s
37 $[HCNH\cdots NF_3]^+$	C_{3v}	(180)	445.71275	0.00739	−0.400	0.478	−0.776	C_s
38 $[LiCNH\cdots NCCN]^+$	$C_{\infty v}$	(180)	284.75761	0.01483	−0.472	0.452	−0.485	C_s
39 $[NNNH\cdots NCS]^-$	C_s	171.5	653.74066	0.02383	−0.556	0.405	−0.601	
40 $[H_3NH\cdots NCCN]^+$	C_{3v}	(180)	241.15590	0.01915	−0.687	0.443	−0.521	C_s
41 $[LiCNH\cdots NHF_2]^+$	C_s	172.6	353.91083	0.02510	−0.478	0.452	0.246	
42[f] $H_3NH\cdots NCS$	C_s	141.3	546.58739	0.16793	−0.672	0.405	−0.563	
43 $OCNH\cdots NCLi$	C_s	176.0	267.55428	0.01575	−0.707	0.407	−0.488	$[C_{\infty v}]$
44 $OCNH\cdots NH_3$	C_s	177.1	223.97519	0.01362	−0.716	0.411	−0.830	$[C_{3v}]$
45 $SCNH\cdots NCH$	C_s	179.3	583.28459	0.01131	−0.577	0.412	−0.413	
46 $SCNH\cdots NCF$	C_s	179.6	682.10392	0.01051	−0.578	0.411	−0.403	
47 $CNH\cdots NCH$	$C_{\infty v}$	(180)	185.74654	0.00979	−0.511	0.401	−0.409	C_s
48 $CNH\cdots NCF$	$C_{\infty v}$	(180)	284.56605	0.00917	−0.511	0.400	−0.400	C_s
49 $NNNH\cdots NCLi$	C_s	164.9	263.62872	0.01333	−0.539	0.373	−0.490	
50 $SCNH\cdots NCCN$	C_s	179.8	674.99372	0.00636	−0.587	0.402	−0.432	
51 $NNNH\cdots NH_3$	C_s	180.0	220.04918	0.01074	−0.542	0.375	−0.819	$[C_{3v}]$, C_1
52 $SCNH\cdots NHF_2$	C_s	171.6	744.14831	0.01342	−0.606	0.403	0.281	
53 $OCNH\cdots NCH$	C_s	164.9	260.65038	0.00722	−0.704	0.384	−0.413	$[C_{\infty v}]$
54 $CNH\cdots NCCN$	$C_{\infty v}$	(180)	277.45658	0.00575	−0.512	0.392	−0.425	C_s
55 $OCNH\cdots NCF$	C_s	177.9	359.47045	0.00716	−0.704	0.384	−0.403	
56 $[LiCNH\cdots NF_3]$	C_{3v}	(180)	452.69520	0.00357	−0.475	0.423	−0.807	C_s
57 $OCNH\cdots NCCN$	C_s	174.9	352.36153	0.00429	−0.701	0.374	−0.423	
58 $NNNH\cdots NCH$	C_s	171.5	256.72625	0.00621	−0.526	0.355	−0.412	
59 $[H_3NH\cdots NF_3]^+$	$[C_{3v}]$	(180)	409.08959	[0.00400]	−0.673	0.415	0.794	$[C_1]$
60 $NNNH\cdots NCF$	C_s	168.1	355.54598	0.00581	−0.525	0.352	−0.406	
61 $NNNH\cdots NCCN$	C_s	174.3	348.43751	0.00340	−0.519	0.343	−0.419	
62 $SCNH\cdots NF_3$	C_s	178.0	842.93768	0.00148	−0.618	0.374	0.835	
63 $CNH\cdots NF_3$	C_{3v}	(180)	445.40115	0.00148	−0.511	0.366	0.837	C_s
64 $OCNH\cdots NF_3$	$[C_s]$	175.4	520.30714	[0.00106]	−0.694	0.347	0.841	$[C_{3v}]$, $[C_1]$
65 $NNNH\cdots NF_3$	$[C_s]$	172.7	516.38374	[0.00078]	−0.506	0.318	0.843	$[C_{3v}]$, $[C_{s,syn}]$, $[C_1]$
66 H_3NH^+	T_d		56.54553		−0.655	0.414		
67 F_3NH^+	C_{3v}		352.77140		0.964	0.458		

[a] NHN bond angle, total electronic energy E (au), energy of formation E_f from component parts (au), net atom charges ϵ (Mulliken, e), and other point-group symmetries in which optimization was attempted. Arranged in the order of increasing D. [b] Optimized configuration of lowest energy. **8**: staggered configuration, NHN = 174.6° is the angle inside the planar $FN_dH\cdots N_a$ arc. **65**, anti. [c] Point-group symmetry. Where proper optimization (no negative frequencies) could not be achieved, the lowest-energy optimization is listed and the corresponding PG symbol is in brackets. [d] (180°) indicates that the angle is 180° by symmetry. [e] $E_f = E(\text{product}) - \sum E(\text{component parts})$. The two component parts are indicated by the dotted bond and are of matching symmetry. [f] [PG] indicates failure to optimized properly in that PG. The other PGs listed resulted in higher energies than that reported in the table. [g] Ring structure with the H-bonds in the ring: **20**, 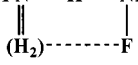 , bifurcated F···2H bond; **42**, 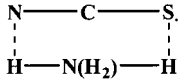 .

TABLE 2: Internuclear and Atom···BCP Distances (Å), Electron Densities $\rho_c(r)$, Laplacians $\nabla^2\rho_c(r)$, Eigenvalues λ_i of the Laplacians, Ellipticities η, and Kinetic Energy Densities $G(r)$ and $K(r)$ at the Bond-Critical Points (all in au) in the 6-31G-Optimized Species of Table 1 (Arranged in the Order of Increasing D)[a]**

	D	d'; d''	x'; x''	ρ'; ρ''	λ_{12}'; λ_{12}''	λ_3'; λ_3''	η	$\nabla^{2'}$; $\nabla^{2''}$	G'; G''	K'; K''
1	2.585	1.119	0.920	0.2579	−1.2429	1.1058	0	−1.3801	0.0472	0.3922
		1.466	1.055	0.0861	−0.2083	0.4899	0	0.0732	0.0566	0.0383
2	2.596	1.093	0.899	0.2390	−1.1414	1.0105	0	−1.2724	0.0452	0.3633
		1.503	1.087	0.0739	−0.1720	0.4292	0	0.0853	0.0494	0.0280
3	2.615	1.086	1.100	0.2482	−1.2038	1.0476	0	−1.3601	0.0434	0.3834
		1.529	0.894	0.0704	−0.1599	0.4161	0	0.0964	0.0473	0.0232
4	2.625	1.073	0.881	0.2610	−1.2581	1.0649	0	−1.4513	0.0442	0.4070
		1.552	1.109	0.0674	−0.1448	0.4026	0	0.1129	0.0466	0.0184
5	2.636	1.065	0.873	0.2589	−1.2190	1.0154	0.000	−1.4227	0.0454	0.4010
		1.571	1.115	0.0619	−0.1219	0.3686	0.001	0.1248	0.0442	0.0130
6	2.639	1.076	0.884	0.2588	−1.2803	1.0823	0	−1.4784	0.0398	0.4093
		1.563	1.114	0.0625	−0.1336	0.3816	0	0.1144	0.0434	0.0148
7	2.647	1.058	0.868	0.2684	−1.2995	1.0739	0	−1.5251	0.0433	0.4245
		1.589	1.126	0.0598	−0.1186	0.3638	0	0.1266	0.0428	0.0111
8	2.649	1.127	0.914	0.2490	−1.0849	0.9130	0.015	−1.2569	0.0493	0.3635
		1.525	1.096	0.0844	−0.1866	0.4373	0.004	0.0642	0.0492	0.0332
9	2.650	1.086	0.894	0.2873	−1.4473	1.2052	0	−1.6893	0.0380	0.4603
		1.564	1.128	0.0623	−0.1430	0.4071	0	0.1212	0.0456	0.0153
10	2.653	1.072	0.884	0.2586	−1.2856	1.0839	0	−1.4873	0.0389	0.4107
		1.581	1.126	0.0601	−0.1276	0.3689	0	0.1137	0.0413	0.0129
11	2.657	1.068	0.875	0.2655	−1.2623	1.0440	0	−1.4806	0.0435	0.4136
		1.589	1.128	0.0623	−0.1234	0.3668	0	0.1199	0.0430	0.0131
12	2.663	1.070	0.870	0.2849	−1.3088	1.0176	0.000	−1.5997	0.0413	0.4412
		1.594	1.116	0.0613	−0.1188	0.3707	0.001	0.1333	0.0434	0.0101
13	2.671	1.055	0.865	0.2767	−1.3358	1.0757	0	−1.5958	0.0403	0.4393
		1.616	1.135	0.0553	−0.1020	0.3360	0	0.1320	0.0403	0.0073
14	2.675	1.070	0.870	0.2851	−1.3086	1.0167	0	−1.6005	0.0413	0.4414
		1.604	1.125	0.0608	−0.1185	0.3686	0	0.1316	0.0426	0.0097
15	2.679	1.059	0.872	0.2671	−1.3345	1.0989	0	−1.5704	0.0370	0.4296
		1.620	1.146	0.0536	−0.1076	0.3353	0	0.1200	0.0374	0.0074
16	2.714	1.050	0.864	0.2780	−1.4140	1.1359	0	−1.6921	0.0339	0.4569
		1.664	1.166	0.0477	−0.0902	0.3025	0	0.1221	0.0338	0.0033
17	2.719	1.047	0.854	0.2852	−1.3624	1.0787	0.000	−1.6462	0.0398	0.4513
		1.673	1.163	0.0495	−0.0837	0.2855	0.030	0.1181	0.0341	0.0046
18	2.729	1.050	0.852	0.2780	−1.2643	0.9906	0.000	−1.5380	0.0434	0.4279
		1.682	1.167	0.0491	−0.0814	0.2780	0.033	0.1146	0.0330	0.0043
19	2.772	1.047	0.854	0.3246	−1.6161	1.2234	0.010	−2.0088	0.0297	0.5319
		1.725	1.183	0.0430	−0.0743	0.2723	0.004	0.1237	0.0308	−0.0001
20	2.787	1.031	0.829	0.3363	−1.5775	1.1216	0.018	−2.0333	0.0307	0.5393
		1.886	1.262	0.0328	−0.0472	0.1907	0.001	0.0963	0.0240	−0.0001
21	2.792	1.064	0.860	0.2934	−1.3256	0.9898	0	−1.6615	0.0384	0.4538
		1.728	1.204	0.0506	−0.0849	0.2782	0	0.1084	0.0320	0.0049
22	2.795	1.024	0.833	0.3077	−1.4865	1.1276	0	−1.8453	0.0361	0.4974
		1.771	1.216	0.0375	−0.0576	0.2304	0	0.1152	0.0277	−0.0011
23	2.815	1.051	0.854	0.3225	−1.5718	1.1903	0.010	−1.9533	0.0320	0.5203
		1.771	1.222	0.0444	−0.0789	0.2635	0.018	0.1057	0.0284	0.0020
24	2.815	1.027	0.836	0.3051	−1.4822	1.1389	0.000	−1.8255	0.0357	0.4921
		1.794	1.244	0.0397	−0.0652	0.2343	0.029	0.1039	0.0267	0.0007
25	2.818	1.023	0.828	0.3029	−1.4110	1.0612	0.000	−1.7605	0.0399	0.4500
		1.796	1.229	0.0352	−0.0520	0.2134	0.000	0.1094	0.0258	−0.0016
26	2.840	1.011	0.820	0.3146	−1.5202	1.1487	0.000	−1.8917	0.0378	0.5108
		1.829	1.249	0.0320	−0.0469	0.1980	0.000	0.1043	0.0238	−0.0023
27	2.850	1.016	0.826	0.3157	−1.5503	1.1670	0.000	−1.9335	0.0325	0.5159
		1.837	1.250	0.0308	−0.0457	0.1924	0.001	0.1010	0.0228	0.0024
28	2.861	1.014	0.822	0.3117	−1.4876	1.1283	0	−1.8469	0.0399	0.5016
		1.847	1.276	0.0358	−0.0524	0.2031	0	0.0983	0.0246	0.0000
29	2.864	1.014	0.824	0.3176	−1.5570	1.1676	0	−1.9464	0.0322	0.5188
		1.850	1.254	0.0292	−0.0421	0.1822	0	0.0979	0.0219	−0.0026
30	2.868	1.040	0.828	0.3098	−1.3251	0.9189	0.023	−1.7313	0.0441	0.4769
		1.828	1.233	0.0369	−0.0513	0.1965	0.054	0.0939	0.0244	0.0009
31	2.881	1.031	0.831	0.3351	−1.5870	1.1351	0.017	−2.0390	0.0299	0.5396
		1.850	1.246	0.0314	−0.0463	0.1923	0.008	0.0997	0.0228	−0.0021
32	2.884	1.052	0.859	0.3244	−1.6291	1.2500	0	−2.0083	0.0279	0.5300
		1.832	1.257	0.0375	−0.0645	0.2215	0	0.0926	0.0232	0.0001
33	2.889	1.030	0.826	0.3268	−1.4833	1.0355	0	−1.9312	0.0338	0.5166
		1.859	1.351	0.0311	−0.0446	0.1876	0	0.0984	0.0227	−0.0019
34	2.895	1.028	0.824	0.3286	−1.4888	1.0346	0	−1.9431	0.0336	0.5194
		1.867	1.252	0.0299	−0.0419	0.1804	0	0.0965	0.0221	−0.0020
35	2.933	1.003	0.807	0.3296	−1.5498	1.1299	0	−1.9696	0.0365	0.5289
		1.930	1.296	0.0256	−0.0336	0.1515	0	0.0842	0.0191	−0.0019

TABLE 2 (Continued)

	D	*d′*; *d″*	*x′*; *x″*	*ρ′*; *ρ″*	λ_{12}'; λ_{12}''	λ_3'; λ_3''	*η*	$\nabla^{2\prime}$; $\nabla^{2\prime\prime}$	*G′*; *G″*	*K′*; *K″*
36	2.940	1.008	0.811	0.3263	−1.5243	1.1153	0	−1.9333	0.0380	0.5214
		1.932	1.316	0.0300	−0.0405	0.1641	0	0.0832	0.0207	−0.0001
37	2.945	1.024	0.836	0.3069	−1.5348	1.1731	0	−1.8966	0.0297	0.5038
		1.921	1.315	0.0277	−0.0424	0.1625	0	0.0776	0.0177	−0.0017
38	2.949	1.008	0.816	0.3254	−1.5793	1.1682	0	−1.9903	0.0319	0.5295
		1.941	1.303	0.0235	−0.0315	0.1427	0	0.0797	0.0176	−0.0022
39	2.961	1.022	0.807	0.3303	−1.3994	0.9217	0.027	−1.8772	0.0445	0.5138
		1.947	1.290	0.0268	−0.0339	0.1496	0.020	0.0818	0.0196	−0.0008
40	2.977	1.023	0.816	0.3246	−1.4984	1.0193	0	−1.9776	0.0335	0.5279
		1.954	1.298	0.0246	−0.0323	0.1439	0	0.0792	0.0181	−0.0017
41	2.977	1.006	0.815	0.3248	−1.5616	1.1568	0.000	−1.9667	0.0334	0.5250
		1.974	1.337	0.0252	−0.0358	0.1439	0.015	0.0728	0.0171	−0.0011
42	2.995	1.020	0.811	0.3376	−1.4870	0.9917	0.006	−1.9823	0.0354	0.5310
		2.130	1.377	0.0202	−0.0182	0.0995	0.552	0.0631	0.0147	−0.0011
43	3.006	1.005	0.799	0.3274	−1.4357	1.0022	0.002	−1.8691	0.0434	0.5107
		2.002	1.328	0.0221	−0.0270	0.1247	0.007	0.0707	0.0163	−0.0013
44	3.008	1.009	0.801	0.3246	−1.4113	0.9832	0.002	−1.8392	0.0488	0.5046
		2.000	1.350	0.0265	−0.0335	0.1383	0.005	0.0714	0.0180	0.0002
45	3.023	0.993	0.797	0.3348	−1.5676	1.1436	0.000	−1.9916	0.0392	0.5371
		2.030	1.346	0.0193	−0.0236	0.1132	0.000	0.0660	0.0148	−0.0017
46	3.038	0.992	0.795	0.3361	−1.5699	1.1425	0.000	−1.9974	0.0394	0.5388
		2.046	1.351	0.0183	−0.0218	0.1068	0.000	0.0631	0.0142	−0.0016
47	3.096	0.992	0.791	0.3432	−1.5666	1.1072	0	−2.0270	0.0383	0.5443
		2.104	1.377	0.0168	−0.0197	0.0954	0	0.0560	0.0129	−0.0011
48	3.102	0.992	0.790	0.3439	−1.5675	1.1056	0	−2.0291	0.0385	0.5458
		2.110	1.376	0.0162	−0.0187	0.0922	0	0.0550	0.0126	−0.0011
49	3.122	1.012	0.787	0.3439	−1.3962	0.8540	0.032	−1.9383	0.0490	0.5336
		2.135	1.375	0.0182	−0.0208	0.0975	0.019	0.0559	0.0135	−0.0004
50	3.128	0.988	0.789	0.3407	−1.5691	1.1294	0.000	−2.0090	0.0407	0.5429
		2.140	1.398	0.0149	−0.0171	0.0850	0.000	0.0508	0.0116	−0.0011
51	3.139	1.014	0.789	0.3414	−1.3822	0.8456	0.032	−1.9182	0.0496	0.5293
		2.125	1.402	0.0218	−0.0255	0.1058	0.018	0.0551	0.0147	0.0009
52	3.158	0.990	0.789	0.3395	−1.5470	1.1078	0.001	−1.9861	0.0418	0.5383
		2.176	1.437	0.0161	−0.0194	0.0870	0.129	0.0482	0.0115	−0.0006
53	3.187	0.997	0.782	0.3391	−1.4285	0.9460	0.003	−1.9110	0.0472	0.5250
		2.214	1.420	0.0135	−0.0150	0.0745	0.006	0.0447	0.0105	−0.0007
54	3.197	0.989	0.784	0.3475	−1.5657	1.0921	0	−2.0394	0.0395	0.5493
		2.208	1.425	0.0131	−0.0147	0.0738	0	0.0443	0.0103	−0.0008
55	3.207	0.997	0.782	0.3394	−1.4213	0.9339	0.003	−1.9087	0.0478	0.5250
		2.210	1.418	0.0135	−0.0149	0.0747	0.007	0.0449	0.0105	−0.0007
56	3.208	0.999	0.802	0.3363	−1.5917	1.1525	0	−2.0309	0.0330	0.5407
		2.210	1.455	0.0141	−0.0171	0.0772	0	0.0430	0.0099	−0.0009
57	3.317	0.995	0.776	0.3424	−1.4141	0.9121	0.004	−1.9161	0.0494	0.5284
		2.325	1.474	0.0106	−0.0114	0.0588	0.005	0.0360	0.0083	−0.0007
58	3.323	1.007	0.774	0.3497	−1.3745	0.7962	0.036	−1.9529	0.0527	0.5409
		2.324	1.462	0.0117	−0.0126	0.0634	0.018	0.0382	0.0089	−0.0006
59	[3.330	1.016	0.802	0.3437	−1.4903	0.9649	0	−2.0156	0.0348	0.5387
		2.284	1.481	0.0131	−0.0153	0.0693	0	0.0387	0.0090	−0.0006]
60	3.332	1.007	0.773	0.3499	−1.3703	0.7889	0.037	−1.9519	0.0531	0.5410
		2.340	1.464	0.0111	−0.0117	0.0608	0.017	0.0372	0.0086	−0.0007
61	3.459	1.006	1.769	0.3512	−1.3587	0.7673	0.039	−1.9502	0.0545	0.5421
		2.456	1.524	0.0086	−0.0089	0.0475	0.017	0.0297	0.0066	−0.0008
62	3.478	0.988	0.778	0.3451	−1.4952	1.0192	0.002	−1.9712	0.0450	0.5378
		2.491	1.586	0.0075	−0.0082	0.0427	0.003	0.0263	0.0058	−0.0008
63	3.494	0.985	0.777	0.3520	−1.5568	1.0663	0	−2.0474	0.0413	0.5531
		2.509	1.594	0.0073	−0.0079	0.0413	0	0.0255	0.0056	−0.0008
64	[3.642	0.993	0.769	0.3453	−1.3946	0.8716	0.004	−1.9175	0.0519	0.5313
		2.651	1.658	0.0054	−0.0056	0.0319	0.008	0.0205	0.0042	−0.0008]
65	[3.793	1.005	0.763	0.3521	−1.3376	0.7343	0.041	−1.9407	0.0567	0.5419
		2.794	1.716	0.0043	−0.0042	0.0250	0.018	0.0165	0.0033	−0.0008]
66		1.012	0.793	0.3490	−1.4856	0.9309	0	−2.0404	0.0357	0.5458
67		1.025	0.827	0.3558	−1.7527	1.2500	0	−2.2534	0.0198	0.5836

[a] Numbering as in Table 1. Upper line, N_d−H bond (single prime); lower line, H···N_a bond (double prime). $\rho' = \rho_c(X')$, $\rho'' = \rho_c(X'')$, $\nabla^{2\prime} = \nabla^2\rho_c(X')$, $\lambda_{12}' = (\lambda_1' + \lambda_2')/2$ etc. Ellipticity $\eta = (\lambda_1/\lambda_2) - 1$.

$= D/2$, which corresponds to the 45° symmetry line in Figure lA. The scatter about this line reflects the departure of the N_dHN_a angles from 180°: the mean deviation from the $D/2$ line is 0.013 Å ($r^2 = 0.989$) but only 0.003 Å when the two outliers **20** and **42** with $N_dHN_a < 145°$ are removed. The *d′* branch of this plot converges with increasing *D* slowly to the limiting value d_0. The *d″* distance increases with *D* at first nonlinearly and then to all intent and purpose linearly. The variation $\partial d''/\partial D = (1 - E)/(1 - 2E)$, $E = \exp[(d_0 - d'')/b]$, which tends to infinity as $d'' \rightarrow d_{sym}$ and to unity as $d'' \rightarrow \infty$, amounts to 1.09 at $D = 3$ Å (corresponding to $d'' \sim 2$ Å) and to 1.005 at $D = 4$ Å (corresponding to $d'' \sim 3$ Å).

The distance $d' = 1.02$ Å, which, in structural comparisons and in the absence of accurate experimental determination, is

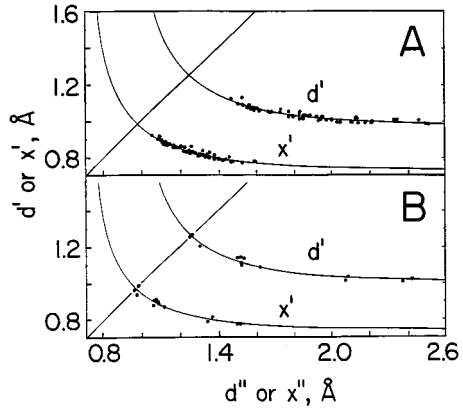

Figure 1. (A) HF data set: regression of d' on d'' according to (1) + (4) and of x' on x'' according to (6). (B) MP2 data set: regression of d' on d'' according to (1) + (4) and of x' on x'' according to (6a). The regression functions are symmetric about the 45° line.

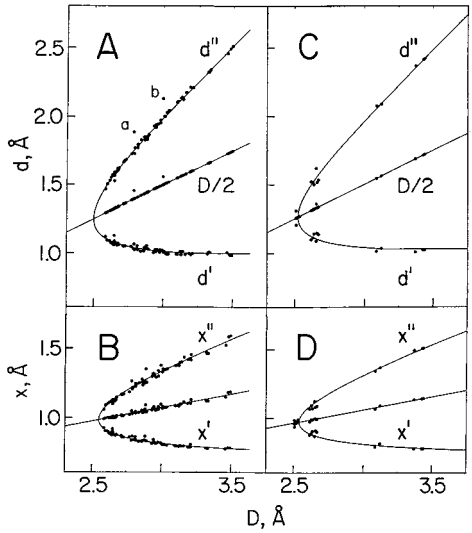

Figure 2. Correlation of d with D for the HF (A) and MP2 (C) data sets and of x with D for the HF (B) and MP2 (D) data sets. The straight lines are the respective $(d' + d'')/2$ and $(x' + x'')/2$ loci. The two outliers *a* and *b* in A represent the d'' of **20** and **42**, respectively, in which NHN < 145°.

often assumed for the length of the N_d−H bond, is reached at $D = 2.91$ Å; for the Steiner set, the corresponding value would be 3.08 Å.

A parallel examination of the d', d'' relationship was undertaken for the MP2-optimized species (Tables 3 and 4, Figures lB and 2C, and text below). This resulted in

$$d_0 = 1.009(8)\ \text{Å},\ b = 0.365(13)\ \text{Å},\ d_{sym} = 1.262(17)\ \text{Å},\ D_{min} = 2.524(34)\ \text{Å} \quad (4a)$$

($r^2 = 0.978$, $\sigma = 0.015$ Å ∼1.4% of range, $r(d_0, b) = -0.95$; Figure lB). The mean deviation from the $D/2$ line in Figure 2C was 0.007 Å, $r^2 = 0.999$. Testing the sums of squares of the residuals showed that, unlike for the HF data set and (1) + (4), representing the MP2 set by (1) + (2) is statistically equivalent to the regression (l) + (4a). The difference between Steiner's model function and (1) + (4a) is everywhere negative. It varies from −0.012 Å at $d'' = 2.5$ Å to −0.004 Å at d_{sym} with a minimum at $d'' = 1.31$ Å and a residual value of ca. −0.013 Å for $d'' > 3$ Å. The MP2 optimization thus overvalues the d', d'', but the MP2-optimized distances are closer to experiment than the corresponding HF values.

The HF optimizations of the very weakly H-bonded **64** and **65** converged, but they resulted in negative frequencies and very large D and d'' values. Here the MP2 optimization was successful: significantly, the D and d'' values it yielded were 0.27−0.37 Å smaller than those from the HF optimizations.

When **59**, **64**, and **65** (for which proper HF optimization could not be achieved) are excluded from the HF and MP2 sets, the difference between D(HF) and D(MP2), statistically, is practically constant and equal to ∼0.12 Å.

While the above d',d'' correlations pertain specifically to N−H−N bonds, without consideration of acceptor atoms other than nitrogen, they can be shown to be consistent with the more comprehensive scheme elaborated for N−H−X bonds;[16] i.e., their validity is not merely local (for a discussion of local vs "universal" relations involving properties at bond-critical points, see ref 17). When the d vs D plot of Figures 2A,C is redrawn as a $d'' - d'$ vs D plot, the resulting curve represents a special case in the family of the $r_1 + r_2$ (→ D) vs $r_1 - r_2$ (→ $d'' - d'$) curves for N−H−X bonds, where X = F, Cl, Br, CN and $r_1 = d$(H···X), $r_2 = d$(N−H).[16] With ab initio (RHF/6-3lG** or better) r_1,r_2 values, the curve for each of the N, X combinations is very well fitted by the generalized form of (3),

$$r_1 + r_2 = 2r_{02} + (r_1 - r_2) + 2b \ln\{1 + \exp[(r_{01} - r_{02} - r_1 + r_2)/b]\} \quad (3a)$$

$$b = [(r_1 + r_2)_{min} - (r_{01} + r_{02})]/(2 \ln 2)$$

r_{01},r_{02} (→ d_0) being the limiting values of r_1, r_2. Our examination of the fitted curves shows that their minima are on a locus approximated by the straight line $(r_1 + r_2)_{min} = 2.538(14) + 1.022(57)(r_1 - r_2)$, $n = 9$, $r^2 = 0.979$, $\sigma = 0.036$ Å ∼6% of range. The $(r_1 + r_2)_{min}$ value estimated for the special case of homoconjugated bonds, i.e., X = N and $r_1 - r_2 = 0$, would thus be 2.538(14) Å, in excellent agreement with the value estimated for D_{min} from (4a) for the MP2 set with Steiner's D_{min} from (2).

The Symmetric N−H−N Bond. Steiner's experimental regression (1) + (2) and Figures 1 and 2 imply that, within the natural variability of the sample set, the conjugate d',d'' distances in linear or near-linear Z_dN_d−H···N_aZ_a bonds are uniquely determined by D and that all such N−H−N bonds are asymmetric except at D_{min} where $d' = d'' = d_{sym}$. A further implication is that *any linear symmetric* ZN−H−NZ bond will, within the regression uncertainty, have the same dimensions, regardless of the nature of Z, i.e., of the particular chemistry of the molecule or ion containing the bond. The centrosymmetric bond in $[4.4.4]^+$, with its $D \sim 2.54$ Å (see above), is a documented example of such a bond. The available evidence[5−7,9] indicates that this, the shortest linear N−H−N bond known, has a single potential minimum.

Given the close agreement between Steiner's experimental regression and that of (1) + (4), convergence to a linear symmetric bond would be expected for the potentially symmetric (= prosymmetric) species of **S** on HF optimization. However, as evident from Figures 1A and 2A, this expectation did not realize.

In Table 1, entries **2**−**5**, **7**, **11**, **21**, **23**, **30**, and **32** are prosymmetric. As the table shows, they all optimized properly but not in point-group symmetries that require symmetric, though not necessarily linear, N−H−N bonds. None of these species has a D value below 2.5 Å (in fact, the smallest D of *any* of the species in **S** is 2.585 Å, in **1**), and their N−H−N bonds are distinctly asymmetric. The position of the H atom in

TABLE 3: MP2/6-31G-Optimized Equilibrium Molecular Geometries of Prosymmetric and Other Selected Species of Table 1[a]**

configuration	PG	N_dHN_a	$-E$	$-E_f$	$\epsilon(N_d)$	ϵ(H)	$\epsilon(N_a)$	other PGs tried
2 $[FCNH\cdots NCF]^+$	$D_{\infty h}$	(180)	384.62456	0.04846	−0.473	0.621	−0.473	$C_{\infty v}$, C_s
7 $[SCNH\cdots NCS]^-$	$C_{\infty v}$	(180)	981.13549	0.04834	−0.459	0.449	−0.474	[$D_{\infty h}$], C_1
4 $[LiCNH\cdots NCLi]^+$	$D_{\infty h}$	(180)	200.55692	0.06488	−0.392	0.483	−0.392	$C_{\infty v}$, C_s
3 $[HCNH\cdots NCH]^+$	$D_{\infty h}$	(180)	186.66584	0.05110	−0.349	0.527	−0.349	$C_{\infty v}$, C_{2v}, C_s, [C_2]
10 $[NCCNH\cdots NCCN]^+$	$D_{\infty h}$	(180)	370.61388	0.03871	−0.443	0.524	−0.443	$C_{\infty v}$, C_1
11 $[CNH\cdots NC]^-$	C_s	180.0	185.75750	0.06025	−0.615	0.532	−0.638	[$D_{\infty h}$], [$C_{\infty v}$], [C_{2v}]
17 $[CNH\cdots NNN]^-$	C_s	177.2	256.97476	0.05069	−0.374	0.396	−0.535	[$C_{\infty v}$]
1 $[F_3NH\cdots NCF]^+$	C_{3v}	(180)	545.66829	0.05940	−0.304	0.512	−0.577	
23 $[F_2HNH\cdots NHF_2]^+$	C_s	176.9	508.83071	0.03307	0.243	0.498	0.130	
20[b] $[FH_2NH\cdots NH_2F]^+$	C_s	157.4	310.98011	0.04388	−0.184	0.446	−0.336	
32 $[F_3NH\cdots NF_3]^+$	C_{3v}	(180)	706.70503	0.02006	0.676	0.500	0.577	[D_{3d}], [C_1]
21 $[H_3NH\cdots NH_3]^+$	C_{3v}	(180)	113.16684	0.04995	−0.708	0.445	−0.814	[D_{3d}], C_1
53 $OCNH\cdots NCH$	C_s	179.7	261.40659	0.00969	−0.575	0.354	−0.319	[$C_{\infty v}$]
59 $[H_3NH\cdots NF_3]^+$	C_{3v}	(180)	409.96801	0.00756	−0.652	0.402	0.609	C_1
64 $OCNH\cdots NF_3$	C_s	176.5	521.46024	0.00275	−0.568	0.324	0.658	[C_{3v}]
65[c] $NNNH\cdots NF_3$, *anti*	C_s	173.3	517.58028	0.00251	−0.418	0.317	0.658	[C_1]
65[c] $NNNH\cdots NF_3$, *syn*	C_s	178.2	517.58028	0.00251	−0.418	0.317	0.658	[C_{3v}]
66 H_3NH^+	T_d		56.73368		−0.631	0.408		
67 F_3NH^+	C_{3v}		353.45819		0.783	0.454		

[a] No negative frequencies. Arranged in the order of increasing D. Numbering, symbols, and abbreviations as in Table 1. [b] Planar ring with F···2H bifurcation. [c] *Syn* with respect to the F atom in the symmetry plane and closing the NNNH···N−F arc.

TABLE 4: Internuclear and Atom···BCP Distances (Å), Electron Densities $\rho_c(r)$, Laplacians $\nabla^2\rho_c(r)$, Eigenvalues λ_i of the Laplacians, Ellipticities η, and Kinetic Energy Densities $G(r)$ and $K(r)$ at the Bond-Critical Points (all in au) in the MP2/6-31G Optimized Species of Table 3 (Arranged in the Order of Increasing D)[a]**

	D	d'; d''	x'; x''	ρ'; ρ''	λ_{12}'; λ_{12}''	λ_3'; λ_3''	η	$\nabla^{2\prime}$; $\nabla^{2\prime\prime}$	G'; G''	K'; K''
2	2.509	1.255	0.983	0.1478	−0.5023	0.5657	0	−0.4388	0.064	0.1736
		1.255	0.983	0.1478	−0.5023	0.5657	0	−0.4388	0.064	0.1736
7	2.510	1.204	0.934	0.1782	−0.6031	0.5964	0	−0.6098	0.070	0.2222
		1.307	0.975	0.1346	−0.3849	0.5481	0	−0.2218	0.069	0.1246
4	2.518	1.259	0.959	0.1566	−0.4948	0.5682	0	−0.4213	0.069	0.1741
		1.259	0.959	0.1566	−0.4948	0.5682	0	−0.4213	0.069	0.1741
3	2.520	1.260	0.964	0.1538	−0.4950	0.5647	0	−0.4253	0.066	0.1727
		1.260	0.964	0.1538	−0.4950	0.5647	0	−0.4253	0.066	0.1727
10	2.524	1.262	0.964	0.1522	−0.4877	0.5588	0	−0.4165	0.066	0.1697
		1.262	0.964	0.1522	−0.4877	0.5588	0	−0.4165	0.066	0.1697
11	2.534	1.267	0.986	0.1491	−0.4828	0.5428	0.000	−0.4228	0.065	0.1703
		1.267	0.986	0.1491	−0.4828	0.5428	0.000	−0.4228	0.065	0.1703
17	2.617	1.097	0.874	0.2487	−1.0144	0.8323	0.001	−1.1966	0.058	0.3571
		1.521	1.065	0.0763	−0.1569	0.4038	0.030	0.0900	0.048	0.0257
1	2.629	1.111	0.886	0.2326	−0.9533	0.8227	0	−1.0840	0.059	0.3294
		1.518	1.091	0.0848	−0.2066	0.4522	0	0.0390	0.047	0.0377
23	2.637	1.139	0.902	0.2480	−0.9996	0.8154	0.008	−1.1839	0.059	0.3547
		1.499	1.069	0.0937	−0.2254	0.4932	0.010	0.0425	0.053	0.0423
20	2.653	1.086	0.865	0.2822	−1.1941	0.9070	0.014	−1.4811	0.051	0.4211
		1.618	1.122	0.0661	−0.1291	0.3723	0.009	0.1142	0.043	0.0139
32	2.659	1.144	0.908	0.2455	−1.0044	0.8349	0	−1.1738	0.057	0.3503
		1.516	1.079	0.0894	−0.2162	0.4760	0	0.0436	0.049	0.0383
21	2.669	1.135	0.897	0.2390	−0.9161	0.7137	0	−1.1186	0.057	0.3366
		1.534	1.087	0.0842	−0.1790	0.4242	0	0.0662	0.048	0.0314
53	3.087	1.011	0.785	0.3240	−1.3009	0.8614	0.008	−1.7403	0.057	0.4925
		2.076	1.343	0.0196	−0.0333	0.1048	0.006	0.0582	0.014	−0.0004
59	3.123	1.032	0.810	0.3233	−1.3424	0.8858	0	−1.7990	0.045	0.4947
		2.090	1.368	0.0209	−0.0267	0.1085	0	0.0551	0.013	−0.0004
64	3.373	1.006	0.772	0.3308	−1.2871	0.8135	0.009	−1.7607	0.062	0.5018
		2.369	1.495	0.0109	−0.0121	0.0581	0.006	0.0339	0.008	−0.0007
65	3.430	1.020	0.773	0.3273	−1.2212	0.7267	0.037	−1.7157	0.065	0.4942
		2.415	1.509	0.0103	−0.0112	0.0546	0.014	0.0319	0.007	−0.0007
65	3.440	1.020	0.773	0.3272	−1.2203	0.7259	0.037	−1.7148	0.065	0.4940
		2.421	1.512	0.0102	−0.0111	0.0537	0.013	0.0315	0.007	−0.0007
66		1.023	0.795	0.3331	−1.3629	0.8594		−1.8665	0.045	0.5119
67		1.042	0.831	0.3317	−1.5195	1.0831		−1.9559	0.031	0.5198

[a] For numbering, symbols, etc. see Tables 2 and 3.

the bond is plotted against D in Figure 3. Interestingly, the resulting d' and d'' in these bonds are well accommodated by the d vs D curve of Figure 2A, and the separation $z = 2d'' - D$ of the two alternative positions of the H atom follows directly from (3) + (4).

When attempts were made to optimize these species in centrosymmetric point groups or in point groups containing C_s(⊥NN) or C_2(⊥NN) symmetry elements (cf. Table 1) and from different parameter estimates, the optimizations converged but resulted in one or more negative frequencies and higher total

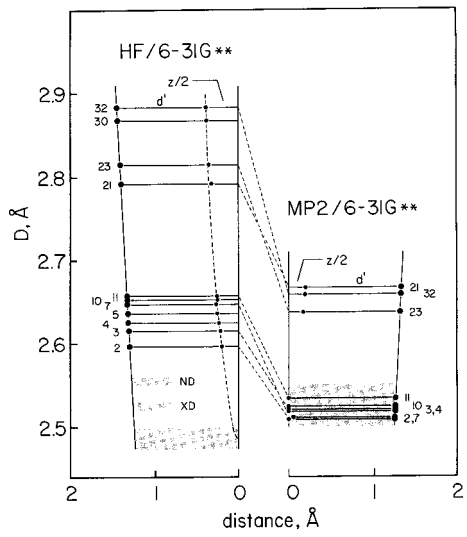

Figure 3. HF (left) and MP2 (right) optimizations of the prosymmetric species: position of the H atom in the linear or near-linear ZN−H−NZ bond plotted against *D*. Large circles: N atoms. Small circles: H atoms. Only one of the alternative positions (relative to the midpoint of the N···N distance) is shown; the two positions are separated by a distance $z = d'' - (D/2)$ (see text). The dashed lines relate the HF-optimized to the MP2-optimized geometries. The shaded bands represent the $D_{min} \pm 1\sigma$ limits as estimated from (4) and (4a), respectively, and the $\pm 1\sigma$ estimated from the experimental *D* values for the shortest known, symmetric N−H−N bond (XD, X-ray diffraction at room temperature; ND, neutron diffraction at 20 K; see text).

electronic energies. However, the *D* values so obtained were significantly closer to the D_{min} estimated from (l) + (4) than the values in the corresponding, properly optimized but asymmetric conformations.

These observations led us to believe that the failure to obtain symmetric N−H−N bonds in the **S** set was an artifact of the HF method and that symmetric bonds might be found in at least some of the above species if their geometries were optimized at a higher level. The prosymmetric species were therefore reoptimized in MP2/6-31G** in several point-group symmetries each, with the lowest energy conformation reported in Table 3.

The pro-$D_{\infty h}$ species **2**−**4** and **10** (but not **5** and **30**) optimized properly under that symmetry. Numbers **7** and **11** each gave one negative frequency in $D_{\infty h}$, but **11** optimized in C_s rendered a geometry indistinguishable from $D_{\infty h}$, while **7**, when optimized in $C_{\infty v}$, remained slightly asymmetric. However, MP2 optimization of **5** and **30**, while convergent, resulted in imaginary frequencies for all the geometries and point groups tried (note that the HF optimizations in C_s were successful (cf. Table 1).

The less strongly H-bonded ($D > 2.65$ Å) *pro*-D_{3d} species **21** and **32**, however, resisted proper MP2 optimization in that symmetry, and their C_{3v}-optimized (staggered) geometries contained unmistakably asymmetric N−H−N bonds. Similarly, optimization of the *pro*-C_{2h} **23** in C_s (pseudo-C_{2h}) resulted in an asymmetric N−H···N bond both in HF and MP2. Since the equilibrium geometries of weakly H-bonded complexes appear to change only insignificantly in post-MP2 optimizations,[18] this asymmetry confirms the validity of the HF results, viz. the (static) N−H−N bonds in **21**, **23**, and **32** *are* asymmetric. This agrees with the expectation from Figure 2A and, for **21**, also with previous[10] ab initio calculations that included varying amounts of correlation effects (lowest $E = -112.87099$ au, smallest $D = 2.73$ Å, $d' = 1.144$ Å; to be compared with −113.166855 au, 2.669 Å, 1.135 Å in **21** (MP2/C_{3v})).[19] For **21**, there are also experimental *D* values for the $N_2H_7^+$ cation from the careful determinations of the crystal structures of several phases of N_2H_7I and N_2D_7I by X-ray (powder and single crystal) and neutron powder diffraction at appropriate temperatures (≥160 K).[21] Comparisons with **21** are complicated by the presence of orientational disorder in some of the phases and by the bond lengthening which is caused by the nonnegligible $N-H^+\cdots I^-$ interactions, but in the phase most suitable for a comparison, the tetragonal N_2H_7I(*II*) at 207 K,[21a] the N···N distance of 2.68(6) Å in the asymmetric cation compares well with the *D*(MP2) in **21**, 2.669 Å.

The relationship between the HF and the MP2 optimizations of the prosymmetric species is displayed in Figure 3. The *D*(MP2) values are all substantially smaller than the corresponding *D*(HF) values, those for **2**−**4**, **7**, **10**, and **11** by 0.09−0.13 Å, those for **21**, **23**, and **32** by 0.13−0.22 Å; i.e., the difference appears to increase roughly linearly with *D*(HF). The *D*(HF) values for the first group on MP2 reoptimization dropped into a band ∼0.025 Å wide, with a *D*(MP2) mean of 2.519(9) Å. This band is well within the $\pm 1\sigma$ range, 2.50−2.55 Å, estimated for the D_{min}(MP2) limit from the *d*′,*d*″ correlation (4a). It is also close to the *D* found for the linear symmetric bond in $[4.4.4]^+$, especially if allowance were to be made for the effect temperature may have on the steric constraint imposed on the bond by the compact cation framework and the crystal environment.

As noted above, the four cations **2**−**4** and **10** optimized in MP2/$D_{\infty h}$ symmetry without difficulty. For the anions **7** and **11**, proper MP2 optimization was not achieved in $D_{\infty h}$ but optimization in lower symmetry resulted in an effectively $D_{\infty h}$ symmetry for **11** and nearly $D_{\infty h}$ for **7**. All of these species contain −C≡N−H−N≡C− as the central group. However, for the anions $[NNN-H-NNN]^-$ (**30**) and $[OCN-H-NCO]^-$ (**5**) the MP2 optimization failed in all the symmetries tried (Table 3), even though the geometries could be optimized as quasilinear asymmetric in HF/C_s. The above results, although limited, seem to suggest that the tendency of prosymmetric species to form symmetric ZN−H−NZ conformations can be related to the type of orbital hybridization on the N atom as determined by the order of the bond(s) between the N atom and the atom covalently attached to it; ionic charge undoubtedly also plays a role. This tendency appears to increase with the order of that bond in the ZN−H donor species. Thus, for ZC≡N−H, the triple bond gives rise to a symmetric bond, while $[Z_3N-H]^+$, at the other end, generates an asymmetric N−H···N bond in the deprotonated dimer.[22] This dependence of the strength, as measured by the internuclear distance, of the unengaged N−H bond in the donor species on bond order parallels that of the C−H bond in gas-phase CH_4, C_2H_4, C_2H_2, and HCN molecules, in which the experimental C−H bond length[23] correlates very well with the bond order *s*: $d(C-H) = 1.0934s^{-0.02907}$, $\sigma = 0.0007$ Å ∼2% of the *d*(C−H) range.

The Symmetric N−H−N Bond: Ab Initio vs Experiment. The long-standing curiosity about the symmetry of short, homoconjugated N−H−N bonds is reflected in the variety of experimental as well as theoretical investigations,[10,20,21,24] even though these are not nearly as numerous as for the corresponding O−H−O bonds. For comparison with the above conclusions from the MP2 optimizations we present results of pertinent crystallographic studies for $D < 2.9$ Å in Figure 4 and Table 5, where z/2 is the displacement of the H atom (or the proton) from the center of the N···N distance. This selection is not as homogeneous as one might wish, since it contains determinations by neutron as well as X-ray diffraction at a variety of temperatures, and it includes, of necessity, bonds with NHN angles stated to be considerably smaller than 180° (Table 5).

TABLE 5: Experimental Data for Homoconjugated (Prosymmetric) ZN−H−NZ Bonds Included in Figure 4[a]

	refcode[b]	method	D, Å	d', Å	d'', Å	NHN	$z/2$[c]	$(z/2)_{corr}$[d]	$\Delta d'$[e]
R	CABMOH, CABMOH01	XD, rt	2.526(3)	1.263	1.263	linear	0		0.03
R	refs 6−8	ND, 20 K	2.556(4)	1.278(3)	1.278(3)	linear	0		0.11
A	BECHOG	XD, rt	2.610(15)	[1.305]	1.305(7)	linear	0		0.18
B	ROHTIR	XD, 200 K	2.62	1.31	[1.31]	linear	0		0.19
C	BEXROL02	XD, 120 K	2.629(4)	1.31	1.31	linear	0		0.20
D	LIJTED	XD, 128 K	2.634(4)	[1.317]	[1.317]	linear	0		0.21
E	BEXROL	ND, 120 K	2.635(2)	1.317(1)	[1.317]	linear	0		0.21
F	ROHTIR	XD, 200 K	2.64	1.32	[1.32]	linear	0		0.21
G	YERLUC	XD, 200 K	2.64	1.24	1.40	175°	0.08		0.13
H	YERLOW	XD, 200 K	2.64	1.19	1.45	179°	0.13		0.08
I	TEHNAV	ND, 100 K	2.644(2)	1.106(5)	1.608(3)	153.5(5)°	0.29	0.25	0.02
J	BEXROL01	XD, rt	2.648(9)	1.29(4)	1.44(4)	152(2)°	0.12	0.08	0.18
K	PATGIA	XD, 193 K	2.650	1.048	1.632	162.3°	0.31	0.29	−0.06
L	APYRDN	ND, rt	2.698(8)	1.17(2)	1.52	177(2)°	0.17		0.08
M	ROHTAJ	XD, 200 K	2.70	1.08	[1.62][f]	175°	0.27		−0.01
N	PYCBZN01	ND, rt	2.737(3)	1.086(7)	1.658(6)	172(1)°	0.29	0.29	0.01
P	CYPYFE	XD, rt	2.74(2)	[1.01][f]	1.86(1)	144°	0.49	0.43	−0.07
Q	HDRZHO11	ND, rt	2.87	1.05	1.83	174°	0.40	0.40	0

[a] This listing, while not exhaustive, is the result of a survey of homoconjugated or near-homoconjugated ZN−H−NZ bonds in the Cambridge Structural Data Base (CSDB). The code letters in the first column refer to Figure 4. The bonds are interpreted as centrosymmetric in A−C, E, F, and R. [b] Reference code in the CSDB. [c] $z/2 = d'' - (D/2)$. [d] $(z/2)_{corr}$ refers to $D_{corr} = d' + d''$ in bonds where NHN < 175°. [e] $\Delta d' = d'_{expt} - d'_{curve}$ (Figure 4). [f] Distance calculated from the NHN angle quoted.

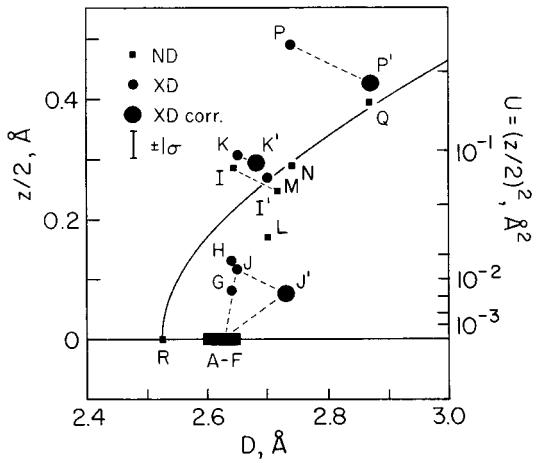

Figure 4. Variation, with D, of the displacement of $z/2$ of the H atom from the center of the N···N distance in homoconjugated (prosymmetric) ZN−H−NZ bonds. The curve represents the ab initio functional relationship expressed from (3) + (4a) and agrees, within its $\sigma \sim 0.02$ Å (the $\pm 1\sigma$ bar), with Steiner's regression (1) + (2) based on neutron diffraction results. For the experimental points A−R see Table 5 and text. The D and $z/2$ values for I, J, K, and P (reported NHN < 175°) have been adjusted (I′, J′, K′, and P′) assuming $D_{corr} = d' + d''$.

Figure 4 shows clearly that the experimental point R and those with $D \geq 2.7$ Å (M, N, Q, and also I′, K′, P′ after adjusting the D and $z/2$ of I, K, P to $D_{corr} = d' + d''$) are well accommodated by the ab initio curve generated by (3) + (4a), with a vertical error width $\pm 1\sigma \sim \pm 0.02$ Å; we recall that this curve is statistically equivalent to the curve that would be obtained from Steiner's regression (1) + (2). However, for bonds with $D =$ 2.60−2.64 Å and interpreted as linear symmetric (A−F; all except D presumed to have the H nucleus on an inversion center), the $z/2$ values deviate from the curve value by ~0.2 Å. For the remaining points G, H, J, and L, the $z/2$ values deviate from the curve by lesser amounts (Table 5). In the face of these experimental values, which converge fitfully toward symmetry as D decreases, to what degree can one have confidence in the applicability of the ab initio curve to short, homoconjugated N−H−N bonds in crystals?

Although the plot of Figure 4 looks confusing, we can show that, acknowledging the obvious differences (isolated static "dimers" at $T \sim 0$ vs ZN−H−NZ fragments embedded in crystals at finite temperatures) and the σ fit of the ab initio curve, the curve and the experimental points are in fact not incompatible if the following is kept in mind. (i) The positions of the N atoms (i.e., the D value) are at least as (X-rays) or equally (neutrons) accurate as the putative position of the H atom. (ii) The above $z/2$ deviations of ~0.2 Å from the curve values for A−F correspond to $U(H)|| \sim 0.05$ Å^2, a value of a magnitude comparable to the $U(H)_{iso}$ or $U(H)||$ quoted for the actual structure refinements. (iii) As is well-known,[24b,25] when, in a structure refinement, the crystal symmetry calls for placing the H atom or the proton in an ZX−H−XZ bond on a crystallographic symmetry element,[26] the possibility that a static or dynamic disorder is present must be considered. Whether the evidence is interpreted in favor of the H atom or the proton as *on* or *off* the symmetry element will depend on the kind and the resolution of the diffraction data, and on the temperature of the experiment (ambient or low; single vs two or more temperatures). While the interpretation of the evidence may depend *critically* on the resolution, this fact has not always received due attention.

The effect of the experimental conditions on the interpretation of the nature of the N−H−N bond in the perchlorate of the $[(quinuclidin\text{-}3\text{-}one)_2H]^+$ cation has been investigated by Rozière et al.[24] (Table 5). The short bond in the 120 K structure, determined both by neutron (E, BEXROL) and X-ray (C, BEXROL02) diffraction, is interpreted as symmetric, with the hydrogen on an inversion center. In the room-temperature structure (X-rays, J, BEXROL0l) the difference Fourier map suggests that the bond is asymmetric and bent (cf. J′), with the H atom in 2-fold disorder. The coalescence of the two maxima in the difference map on cooling (cf. the dashed line from J to C as well as to E in Figure 4), *without significant change in the N···N distance*, seems to be consistent with dynamic disorder, the increased thermal motion at room-temperature forcing the H atom off the N···N line. However, although on the face of it the evidence for BEXROL and BEXROL02 appears to be consistent with a centrosymmetric bond, this interpretation is, to the authors' own admission, not unassailable. Indeed, the rms displacement of the proton along the N···N line, which in BEXROL is stated to be ~0.19 Å, when taken

as $z/2$ would place H on the ab initio curve (consistent with the $d' \sim 1.11$ Å appropriate to the observed $D = 2.63$ Å and $z/2 \sim 0.20$ Å) and thus argue for an asymmetric quasilinear N−H−N bond.

Similar consideration would apply to A, B, D, and F, all interpreted as symmetric, and to the asymmetric G, H, and L, which inclusion of experimental U(H) might raise to the ab initio curve. Without re-refining the original diffraction data (and perhaps not even then) with the H atom placed at the $z/2$ distance estimated from the ab initio curve, it is difficult to say whether in the individual cases (and excepting R) the experimental evidence for the N−H−N bonds put forward as linear in fact supports or militates against the expectation from the $z/2$ vs D correlation of Figure 4. Nonetheless, with this correlation now available and coherent up to $D \sim 3.5$ Å, it would seem worthwhile to use it as a guide in future structure determinations involving such bonds and to design the experiments with a view to corroboration or otherwise of the present conclusions from the ab initio calculations. Reference to this correlation might also avoid assuming inappropriate N−H distances when describing the geometry of N−H−N bonds in cases where direct evidence of the H position is doubtful or lacking (cf. the "standard" neutron N−H bond length of 1.02 Å, which would be applicable only at $D > 4$ Å, i.e., at the margins of hydrogen bonding, cf. for example NOZQUO, SAXBEY).

The plot of Figure 4 is applicable to linear or near-linear N−H−N bonds and does not lend itself to direct comparisons where the bonds are significantly bent. The above adjustment of the D(NHN < 175°) values to $D_{corr} = d' + d''$ would be justified only if the angular dependence of the H-bond strength was small, but the fact that the adjusted points I′, K′, and P′ (though not J′) are closer to the ab initio curve than the corresponding unadjusted points would seem to suggest that the angular dependence is not large.

Position of the Bond Critical Point. The variation of the position of the BCP X′ in the N_d−H bond and of the BCP X″ in the H···N_a bond in the optimized structures of **S** can be displayed in various ways, all of which show that the position of X′ is strongly correlated with the position of its conjugate X″ as well as with d', d'', and D. When the N_d···X′ = x' and X″···N_a = x'' distances are plotted against D (Figure 2B), the means $(x' + x'')/2$ can be represented to a high degree of correlation by

$$(x' + x'')/2 = 0.479(17) + 0.197(6)D \qquad (5)$$

($r^2 = 0.952$, $\sigma = 0.011$ Å ~5% of range). The resulting regression line, which relates the N_d···X′ and X″···N_a branches of the plot, is analogous to the rectilinear diameter of d',d'' in Figure 2A. For the symmetric situation at $D_{min} = 2.49(20)$ Å, $x' = x'' = x_{sym}$ would be 0.97(3) Å. The x' and x'' parameters are thus clearly correlated and closely mimic d' and d''. This is further confirmed by regressing x' on x'' according to (1) as the model function:

$$x' = x_0 - \beta \ln\{1 - \exp[(x_0 - x'')/\beta]\},\ x_0 = 0.734(6)\ \text{Å},\ \beta = 0.356(10)\ \text{Å} \qquad (6)$$

($r^2 = 0.935$ Å, $\sigma = 0.010$ Å ~7% of range, $x_{sym} = 0.981(13)$ Å; Figure 1A). Here $x_0 = x_{sym} - \beta \ln 2$, the limiting distance, represents the effective radius of the N atom in the symmetric N−H−N bond, from which r(H) = 0.27(2) Å is the associated radius of the H atom in the bond.

The *positions* of X′ and X″ in their respective bonds are plotted in Figure 2B: combining (5) and (6) yields a two-valued function of D implicit in x' and x''. For $D > 3$ Å (i.e., $d'' > 2$ Å), the x' and the x'/d' ratio are essentially constant, whereas x'' increases with d''.

The corresponding regressions for the MP2 set (Figures lB and 2D) yield

$$(x' + x'')/2 = 0.482(18) + 0.192D \qquad (5a)$$

($r^2 = 0.983$, $\sigma = 0.009$ Å ~5% of range); $x_{sym} = 0.967$ Å for $D_{min} = 2.524$ Å from (4a) and

$$x_0 = 0.741(16)\ \text{Å},\ \beta = 0.330(24)\ \text{Å},\ x_{sym} = 0.970(33)\ \text{Å} \qquad (6a)$$

($r^2 = 0.948$ Å, $\sigma = 0.018$ Å ~8% of range, $D_{min} = 2.542(86)$ Å, from (5a)). The radius r(H) of the H atom in the symmetric bond is estimated from (4a)+(6a) as 0.29(3) Å, in agreement with the above HF value of 0.27(2) Å.

The difference between the D_{min}(HF) values calculated from (4) and from (5) + (6), respectively, is well within the joint standard error of the two values, as is the difference between the D_{min}(MP2) values calculated from (4a) and from (5a) + (6a), respectively.

Electron Densities

Electron Density ρ_c at the BCP: The HF Set. While the above functional relationships between the internuclear distances in N−H−N bonds derive from Pauling's (semiempirical) bond-order equation, no such guiding principle appears to have been formulated for representing the variation of the electron density ρ_c at the BCP with d. Descriptions of the observed d,ρ_c dependence are therefore of necessity empirical, and their relative merits have to be judged largely on statistical criteria. A plot of $\rho' = \rho_c$(X′) at the BCP X′ and $\rho'' = \rho_c$(X″) at the BCP X″ against the corresponding d' and d'' suggests that the variation of ρ_c, which spans almost 2 orders of magnitude, is continuous and representable by a simple model function, for which $\rho'' \rightarrow 0$ as $d'' \rightarrow \infty$.

The two simplest such functions are the power function

$$\rho_c = ad^{-b} \qquad (7)$$

and the exponential function

$$\rho_c = a \exp(-bd) \qquad (8)$$

Regressions (not linearized) according to (7) and (8) yielded the parameters listed in Table 6. For the HF set (R71 and R81), the r^2 and σ values indicate that the d,ρ_c are highly correlated. The adequacy of representing this data set by either model function might thus not be called in question and the matter might rest there. However, further inspection reveals that the residuals $\Delta\rho_c = \rho_c$(tabulated) − ρ_c(regression) are not distributed uniformly. The $\Delta\rho'$ in the d',ρ' subset range approximately from −0.013 to 0.039 au for R71, and approximately from −0.018 to 0.031 au for R8l, whereas $\Delta\rho''$ in the d'',ρ'' subset range approximately from −0.008 to 0.010 au for R71 and approximately from −0.008 to 0.014 au for R8l; the nonuniformity of the error variance is shown, in logarithmic presentation, in Figures 5A,C. Thus, the adequacy of representing the HF d,ρ_c data set by (7) or (8) cannot be assessed on the strength of r^2 and σ alone.

The uniformity of the error variance improves when the nonlinear regression functions (7) and (8) are replaced by the

TABLE 6: Regressions of the Electron Density ρ_c at the BCP on the N—H Distances[a]

	data set[b]	n	*a*	*b*	r^2	σ	%[c]	$r(a,b)$[d]
			Power Function, Eq 7					
R71	HF, all	124	0.345(2)	3.65(7)	0.992	0.0127	3.6	0.396
R72	HF, d', ρ' only	63	0.340(3)	2.90(21)	0.768	0.0159	13.6	0.623
R73	HF, d'', ρ'' only	61[e]	0.441(20)	4.25(9)	0.982	0.0029	3.7	0.981
R74	MP2, all	31	0.355(5)	3.50(10)	0.990	0.0107	3.3	0.653
R75	MP2, d', ρ' + *sym*	19	0.355(6)	3.46(18)	0.967	0.0139	7.5	0.707
R76	MP2, d'', ρ'' + *sym*	17[e]	0.342(15)	3.46(15)	0.990	0.0058	4.0	0.946
R77	MP2, all − *sym*	26	0.355(5)	3.42(12)	0.991	0.0117	3.6	0.608
R78	MP2, d', ρ' − *sym*	14	0.348(6)	3.08(24)	0.942	0.0128	8.3	0.717
R79	MP2, d'', ρ'' − *sym*	12[e]	0.385(35)	3.71(23)	0.982	0.0059	4.7	0.964
			Exponential Function, Eq 8					
R81	HF, all	124	2.69(32)	2.82(5)	0.993	0.0115	3.3	0.997
R82	HF, d', ρ' only	63	5.59(12)	2.80(2)	0.770	0.0150	12.8	1.000
R83	HF, d'', ρ'' only	61[e]	2.86(25)	2.41(5)	0.982	0.0028	3.6	0.995
R84	MP2, all	31	6.28(62)	2.90(9)	0.999	0.0110	3.4	0.996
R85	MP2, d', ρ' + *sym*	19	7.78(120)	3.10(14)	0.972	0.0127	6.9	0.997
R86	MP2, d'', ρ'' + *sym*	17[e]	2.76(24)	2.30(7)	0.996	0.0036	2.5	0.995
R87	MP2, all − *sym*	26	5.46(55)	2.76(9)	0.993	0.0108	3.3	0.995
R88	MP2, d', ρ' − *sym*	14	6.00(14)	2.85(21)	0.945	0.0125	8.1	0.999
R89	MP2, d'', ρ'' − *sym*	12[e]	2.87(43)	2.32(10)	0.993	0.0038	3.1	0.995

[a] Direct regression, not via the logarithmically transformed function. [b] *sym* indicates symmetric N−H−N. [c] σ as percentage of the respective ρ_c range. [d] Correlation coefficient for the regression coefficients *a* and *b*. [e] Data set does not include NH_4^+ (**66**) and F_3NH^+ (**67**).

logarithmic versions of these functions

$$\ln \rho_c = \ln a - b \ln d \tag{7a}$$

($r^2 = 0.994$, $a = 0.354$, $b = 3.949$, $\sigma = 0.0974$ ~2.5% of the ln ρ_c range) and

$$\ln \rho_c = \ln a - bd \tag{8a}$$

($r^2 = 0.994$, $a = 4.610$, $b = 2.644$, $\sigma = 0.0980$ ~2.6% of range). Since the ranges of $\Delta\rho'$ and $\Delta\rho''$ in R71 and R81 correspond roughly to the same fraction (5−10%) of the respective ρ' and ρ'' values, it can be argued that the logarithmic functions (7a) and (8a) are more appropriate regression functions than (7) and (8). In any event, it is clear that the inherent scatter of the d',ρ' and d'',ρ'' data points is the factor that limits further improvement in the fit by any single monotonic regression function.

The absence of data points in the interval between the two subsets raises the following question: Is representing the d,ρ_c correlation by a *single* smooth, continuous function, such as (7) or (8), in fact warranted by the data set, or is the correlation represented better by *two* separate such functions, one for each subset? In Table 6, the power regression R71 is contrasted with R72 and R73, and the exponential regression R81 is contrasted with R82 and R83. From the σ values for R73 and R83, it is evident that the d'',ρ'' correlation is represented better by a separate regression, while for the d',ρ' correlation the fidelity of the separate regression is inferior to that achieved by a single global function R71 or R8l. Statistical tests on the sums of squares of the residuals show that the two separate regressions taken jointly fit the data set significantly better than the corresponding single-function regressions, and this is seen directly on rectifying the regression lines in Figure 5, where R71−R73 and R81−R83 are presented as logarithmic transformations ln R71 to R73 and ln R81 to ln R83. Furthermore, the uniformity of distribution of the residuals is significantly improved when two functions are used (Figure 6).

Additional improvement in the goodness of fit and the uniformity of distribution of the residuals results when, instead of the direct regressions (7) and (8) (or their logarithmic transformations), logarithmic regressions are used for the two subsets. This is analogous to what is observed for the single-function logarithmic regressions (7a) and (8a) and supports the view that the logarithmic regressions represent the d,ρ_c correlation more faithfully.

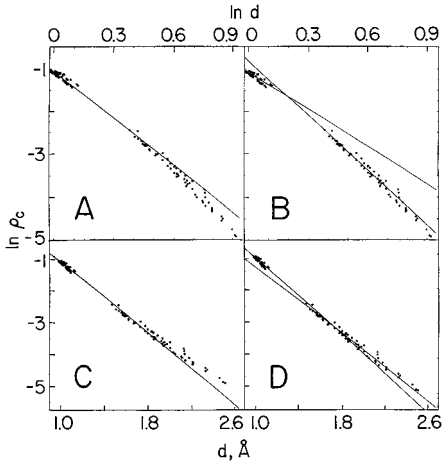

Figure 5. Fitting the HF d,ρ_c data set to a single (A) and to two (B) power functions and to a single (C) and to two (D) exponential functions. The rectified correlation lines represent the logarithmically transformed correlation functions R71−R73 and R81−R83, respectively, of Table 6.

The single-function representation can be rejected, at a >99.5% significance level, in favor of the corresponding two-function representation for both the logarithmically transformed regressions of Table 6 and for the logarithmic regressions, power as well as exponential. Thus, of the representations examined above, the two-function logarithmic regressions represent the HF d,ρ_c correlation best. It should be noted, however, that while the single-function power regression R71 overestimates the ρ_c values for large d (Figure 5A), the corresponding exponential R81 regression underestimates them (Figure 5C). This would suggest that a hybrid model function which combines (7) and (8), $\rho_c = \alpha(7) + (1 - \alpha)(8)$, or the corresponding logarithmically transformed functions, might improve the fit overall and specifically for d'',ρ''. Indeed, the sum $\rho_c = (\ln R71 + \ln R81)/2$ (i.e., $\alpha = 0.5$) gives a lower σ value than either ln R71 or ln R81, and optimizing α might produce a fit better still. However, vis-à-vis the simple functions such composite model functions

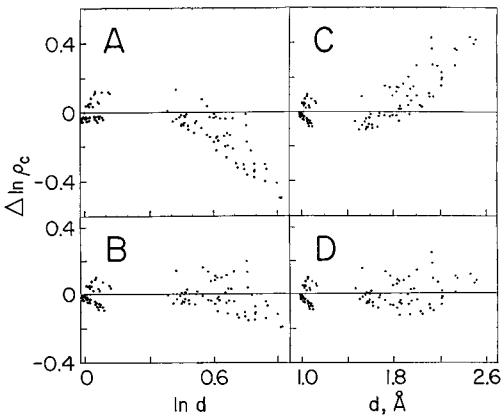

Figure 6. Distribution of the residuals when the correlation of ρ_c and d for the HF set is represented by a single (A) and by two (B) power functions and by a single (C) and by two (C) exponential functions. The residuals $\Delta\ln \rho_c = \ln \rho_c$(tabulated) − $\ln \rho_c$(calculated) correspond to Figure 5, i.e., to logarithmically transformed regression equations R71−R73 and R81−R83, respectively, of Table 6.

appear somewhat contrived and have not been investigated further.

Regressing ρ_c on d does not take account of the pairwise relationship of d' to d'' and of ρ' to ρ''. This neglect of the conjugate nature of d',d'' and ρ',ρ'' is remedied by taking the ratios d'/d'' and ρ'/ρ''. For the single functions

$$\ln(\rho'/\rho'') = b \ln(d''/d') \quad (7b)$$

$$\ln(\rho'/\rho'') = b\,(d'' - d') \quad (8b)$$

These ratios contain only one parameter to be evaluated and implicitly satisfy the requirement that for *symmetric* N−H−N bonds (not present in the HF set) $\rho'/\rho'' = d''/d' = 1$; i.e., the regression line is constrained to pass through the origin. However, for *two* regression functions

$$\ln(\rho'/\rho'') = \ln(a'/a'') + (b'' - b')\ln d'' + b' \ln(d''/d') \quad (7c)$$

$$\ln(\rho'/\rho'') = \ln(a'/a'') + (b'' - b')d'' + b'\,(d'' - d') \quad (8c)$$

and the regression plane in the three-dimensional plot does not pass through the origin.

This and the goodness of fit of (7c) and (8c) can be used as another test of the single- vs two-function hypothesis. Thus, for (7b) we obtain by iteration $b = 3.925$, σ(7b) = 0.1119 ~4.0% of range; for (8b), $b = 2.674$, σ(8b) = 0.1187 ~4.2% of range. For the two-function model, regressing ρ'/ρ'' on d''/d' and d'' according to (7c) yields

$$\ln(\rho'/\rho'') = -0.57(57) + 2.56(99)\ln d'' + 2.15(82)\ln(d''/d'), \quad (7d)$$

where $r^2 = 0.985$, σ(7d) = 0.0914 ~3.3% of range; similarly, ρ'/ρ'' regressed on $d'' - d'$ and d'' according to (8c) yields

$$\ln(\rho'/\rho'') = 2.20(120) - 1.75(73)d'' + 4.00(65)(d'' - d') \quad (8d)$$

where $r^2 = 0.987$, σ(8d) = 0.0855 ~3.1% of range. Thus, while the absolute terms in (7d) and (8d) are nonzero, their error estimates do not preclude the possibility that the regression planes do pass through the origin and the test for the HF set is inconclusive.

For $d' = d''$, i.e., for the symmetric N−H−N bonds and with d_{sym} = 1.249(9) Å from (4), the two-function representation implies that $\rho'/\rho'' = 1.00(2)$ for the power fit and 1.07(2) for the exponential fit. These values would be 1.04 and 1.20, respectively, if the a and b were taken from Table 6. Conversely, for $d' = d''$ and $\rho' = \rho''$ simultaneously, d_{sym} would be 1.25 Å for (7d) and 1.30 Å for (8d), values equivalent within the overall statistics.

Electron Density ρ_c at the BCP: The MP2 Set. The above results for the HF set can be compared with an analogous treatment of the MP2 set. While the d and ρ_c values in the MP2 set might be expected to be more realistic, their number is considerably smaller and their distribution over the d' and d'' ranges is not as uniform as in the HF set. However, they afford an opportunity to examine the effect of inclusion of the symmetric N−H−N bonds on the correlations.

The representations R74 and R84 of the d,ρ_c data set (including the symmetric bonds) by a single function each are statistically equivalent, as are the logarithmic transformations ln R74 and ln R84 of these regression equations and also the *logarithmic* regressions of ln ρ_c on ln d and of ln ρ_c on d (cf. (7a) and (8a)); of these, the ln ρ_c on d regression yields the most uniform distribution of the residuals. However, comparing ln R74 with the corresponding logarithmic regression ln ρ_c on ln d reveals that these two sets are not statistically equivalent, and similarly for ln R84 and the logarithmic regression ln ρ_c on d, the logarithmic regression being significantly better.

In comparing the MP2 results with those for the HF d,ρ_c set, it is appropriate to exclude the symmetric cases from the MP2 set (sets R77 and R87). Here, the error variance ratio for the logarithmically transformed R81 and R87 equations (ln R81 and ln R87) shows that these two regressions are statistically equivalent (at the 95% significance level), whereas the ln R71 and ln R77 are not; the *logarithmic* regressions ln ρ_c on ln d for the two sets are equivalent, but the corresponding regressions ln ρ_c on d for the two sets are not. For the H···N_a end of the ρ_c vs d correlation, testing the MP2 d'',ρ'' subset against the HF d'',ρ'' subset (R73 and R79, and R83 and R89) shows statistical equivalence of ln R83 vs ln R89 but not of ln R73 vs ln R79. The *logarithmic* regressions of ln ρ'' on ln d'', and of ln ρ'' on d'', are statistically equivalent for both the HF and the MP2 sets.

Turning now to the effect of inclusion of the symmetric N−H−N bonds (absent in the HF set), we compare the single-function regressions R74 with R77 and R84 with R87 (Table 6). Within the data range, the maximum difference between R74 and R77 is well within a single σ of either regression, and similarly for R84 and R87. The logarithmically transformed regression equations ln R74 and ln R77 are statistically equivalent but ln R84 and ln R87 are not; the logarithmic regressions, however, are equivalent for both the power and the exponential model functions. There is thus no strong evidence that the MP2 set with the symmetric N−H−N bonds included is statistically different from the MP2 set with the symmetric cases omitted.

The question still remains whether the two-function model represents our MP2 data better than the single-function regressions. For the MP2 set with the symmetric cases excluded (R78 and R79, and R88 and R89) the comparison would mirror that for the HF set, but for the inclusive MP2 set (R75 and R76, and R85 and R86) the comparison is more problematic in that the two sets being compared are not mutually exclusive (Table 6). The results for the logarithmically transformed regression equations of Table 6 (ln R77 vs ln R78 and ln R79; ln R87 vs

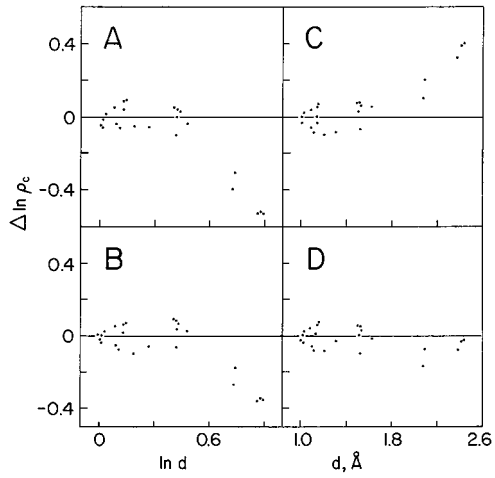

Figure 7. Distribution of the residuals when the correlation of ρ_c and d for the MP2 set (excluding the symmetric bonds) is represented by a single (A) and by two (B) power functions and by a single (C) and by two (C) exponential functions. The residuals $\Delta\ln\ \rho_c = \ln\ \rho_c$(tabulated) $-\ \ln\ \rho_c$(calculated) correspond to Figure 5, i.e., to logarithmically transformed regression equations R77−R79 and R87−R89, respectively, of Table 6 and can be compared to those for the HF set in Figure 6.

ln R88 and ln R89) are presented in Figure 7. The distributions of the residuals are similar to those for the HF set (Figure 6). The ρ'' values again are underestimated in the single-function power regression and overestimated in the single-function exponential regression, i.e., this feature is retained in the MP2 optimizations. The two-function representations are significantly better than the corresponding single-function best fits at a >99.5% significance level.

The single-function *logarithmic* regressions with the symmetric cases omitted are better fits than the corresponding logarithmically transformed power or exponential regressions at a > 99.5% significance level but can be rejected in favor of the two-function logarithmic regressions at the same significance level. However, the separate logarithmic regressions for d',ρ' and d'',ρ'' are statistically equivalent to the corresponding logarithmically transformed regressions (Figures 7B,D), with slightly smaller residuals. The best representation of the d,ρ_c correlation for the (MP2 − *sym)* set is

$$\ln \rho' = -1.060 - 3.123 \ln d',\ r^2 = 0.925,\ \sigma = 0.0559 \sim 9\%\ \text{of range}$$

$$\ln \rho'' = -0.640 - 4.448 \ln d'',\ r^2 = 0.994,\ \sigma = 0.0790 \sim 3\%\ \text{of range} \quad (7e)$$

for the power, and

$$\ln \rho' = 1.810 - 2.875\, d',\ r^2 = 0.930,\ \sigma = 0.0539 \sim 9\%\ \text{of range}$$

$$\ln \rho'' = 1.145 - 2.387\, d'',\ r^2 = 0.997,\ \sigma = 0.0381 \sim 1.5\%\ \text{of range} \quad (8e)$$

for the exponential regression.

These two representations are statistically equivalent to the logarithmically transformed regressions of the $\rho' + \rho_{sym}$ subset on the $d' + d_{sym}$ subset (ln R78 and ln R88) and of the $\rho'' + \rho_{sym}$ subset on the $d'' + d_{sym}$ subset (ln R76 and ln R86), and in turn equivalent to the corresponding logarithmic regressions of these subsets. Overall, the best representation of the MP2 d,ρ_c correlation is

$$\ln \rho' = 2.106 - 3.154\, d',\ r^2 = 0.977,\ \sigma = 0.0496 \sim 6\%\ \text{of range}$$

$$\ln \rho = 1.116 - 2.374\, d'',\ r^2 = 0.998.\ \sigma = 0.0526 \sim 2\%\ \text{of range}, \quad (8f)$$

with the two regression lines intersecting at $d \sim 1.27$ Å, i.e., close to the $d_{sym} = 1.26(2)$ Å value from eq 4a.

As discussed above, analysis of the ρ'/ρ'' vs d''/d' correlation can be used to decide between the single- and the two-function models. While for the HF set the result was inconclusive, it was thought that a clearer picture might emerge for the MP2 set, despite the smallness of the latter. Iterative solution to (7b) gave $b = 3.897$, $r^2 = 0.996$, $\sigma = 0.0887$ ~2.6% of range ($r^2 = 0.992$, $\sigma = 0.1061$ with the symmetric values excluded); and to (8b), $b = 2.539$, $r^2 = 0.997$, $\sigma = 0.0613$ ~2% of range ($r^2 = 0.995$, $\sigma = 0.0740$ with the symmetric cases excluded). The power regression is statistically equivalent, at the 95% significance level, to that for the HF set, but the exponential is not.

Regression according to (7c) resulted in

$$\ln(\rho'/\rho'') = -0.74(20) + 3.16(48) \ln d'' + 1.65(36) \ln(d''/d') \quad (7g)$$

$r^2 = 0.999$, $0 = 0.0393$ ~1% of range; and in

$$\ln(\rho'/\rho'') = -0.63(46) + 2.46(90) \ln d' + 2.24(72) \ln(d''/d') \quad (7h)$$

$r^2 = 0.999$, $\sigma = 0.0454$ ~1.5% of range, with the symmetric cases excluded. Similarly, regression according to (8c) gave

$$\ln(\rho'/\rho'') = 1.62(42) - 1.29(28) d'' + 3.57(23)(d'' - d') \quad (8g)$$

$r^2 = 0.999$, $\sigma = 0.0380$ ~1% of range; and

$$(\rho'/\rho'') = 2.33(97) - 1.91(60) d'' + 4.12(53)(d'' - d') \quad (8h)$$

$r^2 = 0.998$, $\sigma = 0.0436$ ~1.5% of range, with the symmetric cases excluded. Consideration of the error estimates on the absolute terms shows that the regression planes for the full MP2 set, (7g) and (8g), do not pass through the origin; i.e., these representations clearly favor the two-function model; also, their σ values are the lowest.

Neither (7g) nor (7h) is statistically equivalent to the corresponding HF regression (7d), and similarly neither (8g) nor (8h) is statistically equivalent to (8d).

Electron Density ρ_c at the BCP: Conclusions. So far, we have not considered the question of preference between the power and the exponential regression. In most of the power/exponential regression pairs the r^2 and σ values are similar. However, because of the nonlinearity of (7) and (8), statistical equivalence of the two regressions in any given case cannot be established from the r^2 and σ values alone, nor by any *simple* statistical decision rule. Generally, and on the face of it, the exponential model function generates somewhat better figures of merit, but an elaboration of more stringent comparison criteria is not contemplated here. The suitability and relative merits of the logarithmic model functions (7a) and (8a) have been investigated by Alkorta et al.,[28] who examined ab initio d',ρ_c values in 24 N−H bonds and also in a variety of other X−H bonds, X = H, C, O, F, Cl, Br. While the differences in the

composition of the N−H data sets preclude a detailed comparison of the Alkorta regressions with ours, the regression coefficients in (7a) and (8a) are quite similar to those in the Alkorta study, the individual differences not exceeding ∼2% of the respective values except for *b* in (7a), for which the difference was ∼8%. These authors, too, conclude that both model functions represent their data sets more or less equally adequately, though slightly better results were obtained with the exponential model. They also note that the exponential but not the power function is consistent with the exponential falloff of ρ with distance in atoms and molecules.[29]

The approximate range of ρ_c is 0.007−0.35 au in the HF sample and 0.01−0.33 au in the MP2 set. The lower bound of ρ'' is of course zero, while the upper bound of ρ' would be that in *externally unengaged* N−H bonds (ρ_c in au):

	ρ_c(MP2)	ρ_c(HF)	difference	ratio
H_3N	0.349	0.358	0.009	1.026
$H_3NH^+\cdots F^-$	0.349	0.357	0.008	1.023
$H_3N\cdots HNC$ (**36**)	0.348	0.357	0.009	1.026
$H_3NH^+\cdots CN^-$	0.348	0.357	0.009	1.026
HNC	0.341	0.354	0.013	1.038
H_4N^+ (**66**)	0.333	0.349	0.016	1.048
F_3NH^+ (**67**)	0.332	0.356	0.024	1.072

Indeed, the largest ρ' in the HF sample are grouped about $\rho' \sim$ 0.35 au (mean of the $\rho' > 0.34$ au values in Table 2, 0.346(4) au), and in the MP2 sample, about $\rho' \sim 0.33$ au (mean of the $\rho' > 0.32$ au values in Table 4, 0.327(3) au). It appears unlikely that, in isolated model species, linear or near-linear N−H···N bonds will be found with d' significantly below 0.98 Å and ρ' significantly above the ρ_c values in the preceding table, regardless of purposeful manipulation. Even in pertinent *real* crystals at high pressure it is improbable that such bonds would exist, as shorter N−H bonds would require longer H···N bonds, i.e., the donor species would be increasingly non-H-bonded; instead, stronger and bent H-bonds would be expected (solid ammonia at high pressure would be a case in point[30]). To place these ρ_c(NH) values in a larger context, we may contrast them with the ρ_c in a very strong covalent bond. In the N_2 molecule (d(N−N) = 1.094 Å from experiment), ρ_c(HF) ∼ 0.711 au and ρ_c(MP2) ∼ 0.632 au. These values must be very close to the respective (unknown ?) upper ρ bond in *any* type of chemical bond.

In sum, our examination leads to the conclusion that the d,ρ_c correlation is represented, both in the HF and the MP2 set, significantly better by two, rather than a single, power or exponential functions. It is conceivable that a *single* smooth, continuous model function exists that may represent the correlation equally well, but if it does, it has not yet been formulated.

On reflection, the apparent preference for the two-function model to represent the d,ρ_c correlation is not unexpected, given the difference in the nature of the N−H and H···N bonds at large $N_d\cdots N_a$ separations. This difference decreases with decreasing *D*, but the character of the convergence toward the symmetric N−H−N bond from opposite sides, the covalent and the H-bonded, is not the same, as reflected in the unequal dependence of ρ' on d' and of ρ'' on d''. Thus, for the two-function model, $\rho' = \rho''$ at $d_{sym} = d' - d''$, but $d\rho'/dd' \neq d\rho''/dd''$.

The HF set, on one hand, does not lend itself to investigation of smooth continuity of the d,ρ_c correlation, for the sizable gap it contains between $d'(HF)_{max} \sim 1.13$ Å and $d''(HF)_{min} \sim 1.47$ Å is not populated (cf. Figures 5−7) and so d,ρ_c pairs in the vicinity of d_{sym} and at d_{sym} itself are not accessible. As discussed above, HF optimization of prosymmetric species never reached symmetric N−H−N geometries, and attempts to reduce the gap by goal-oriented manipulation of the chemistry of the non-prosymmetric species were not successful. The MP2 set, on the other hand, does contain species with optimized symmetric N−H−N geometries, but the density of d,ρ_c points in the d_{sym} region is not sufficient to define the shape, on the two sides, of the convergence of the d,ρ_c regression function to d_{sym}.

A more determined effort to expand the MP2 set, even if only by reoptimizing additional species of Table 1, may well help to elucidate the nature of the N−H−N d,ρ_c correlation, but ultimately an (as yet unspecified) more realistic and comprehensive set of optimized ab initio geometries will be required to resolve the problems brought to light by the present investigation. The ab initio approach seems at present to show more immediate promise of success than reliance on an eventual accumulation of a sufficiently large, well-conditioned set of *experimental* results: even for O−H−O bonds, for which more abundant experimental results exist, extraction of reasonably accurate d,ρ_c values poses problems, especially at and in the vicinity of d_{sym} (cf. above).[13b,31] As well, it may not be possible to realize, experimentally, N−H−N containing systems expected to have very short, though not necessarily symmetric N−H−N bonds, as such systems may have energetically and structurally more favorable chemical alternatives of no interest in the present context. This restrictive access to short N−H−N bonds has implications for the ρ_c related quantities such as the Laplacian at the BCP; these will be discussed in a subsequent paper.

Summary and Outlook

Analysis of the geometries of linear or near-linear N−H···N bonds in 67 molecular species with geometries optimized at the RHF/6-31G** level (the HF set) and in 19 species optimized at the MP2/6-31G** level (the MP2 set) confirm that the d' = N−H and d'' = H···N distances in a bond are correlated (equations (1)+(4) and (l)+(4a), respectively). The d', d'' correlation for the MP2 set is statistically equivalent to Steiner's regression (1) + (2) based on the results of 19 neutron diffraction studies, which inspires confidence in the ab initio d',d'' values and in the model function. The correlation also makes it possible to estimate the position of the H atom in an N−H···N bond from the N···N distances. This is of practical consequence to the experimentalist, since in structure determinations by X-ray diffraction the positions of the N atoms generally are reliably known, whereas that of the H atom may not be; in structure determinations by neutron diffraction the correlation can be used to verify the experimentally determined position of the proton. These applications are particularly important when the N−H···N bond is short and close to symmetric. The question of whether *all* linear symmetric N−H−N bonds have essentially the same dimensions, as predicted by the d',d'' correlation, is open to further enquiry by extending the existing MP2 and exploring post-MP2 calculations, and by making an effort to realize additional symmetric or near-symmetric N−H−N bonds by experiment.

The positions of the bond critical points x' and x'' in an N−H···N bond also are correlated. The correlation function resembles that for d'/d'' (eqs (6) and (6a), and Figures 2B,D); furthermore, $x' + x'' = c_0 + c_1 D$.

No theoretically based functional dependence of the electron density ρ_c at the BCP appears to have been proposed, hence the uncertainty about the relative suitability of the individual model functions tried. While fitting the d,ρ_c pairs by a single

power (7) or exponential (8) function yields acceptable regressions for both the HF and the MP2 set,[32] neither function accommodates the d',ρ' and d'',ρ'' as well as a combination of *two* functions of the same type, one for the N−H and another for the H···N bonds, i.e., the variation of ρ_c with d over the entire d range appears to be continuous but not smooth (Figure 5). It remains to be seen whether this finding is universally valid and verifiable by ab initio calculations at levels beyond the scope of the present investigation as well as by experiment or whether it is specific to our particular data sets. Alternatively, it may be possible to construct a regression function that fits the d,ρ_c data satisfactorily and is continuous and smooth but incorporates terms additional to those in (7) and (8). This empirical possibility bears investigating in the future unless, or until, a proper *theoretical* basis for the d,ρ_c variation has been established.

Acknowledgment. We thank Drs. T. S. Cameron, D. C. Hamilton, K. N. Robertson, and P. D. Wentzell for the assistance they kindly provided in the course of this investigation. Financial support from the Natural Sciences and Engineering Research Council of Canada is acknowledged.

References and Notes

(1) Jeffrey, G. A. *Cryst. Rev.* **1995**, *4*, 213.

(2) Steiner, T. *J. Chem. Soc., Chem. Commun.* **1995**, 1331.

(3) Pauling, L. *The Nature of the Chemical Bond*, 3rd ed.; Cornell University Press: Ithaca, New York, 1960.

(4) (a) Knop, O.; Choi, S. C.; Hamilton, D. C. *Can. J. Chem.* **1992**, *70*, 2574. (b) Hamilton, D. C.; Knop, O. *Appl. Stat.* **1998**, *47*, 173.

(5) (a) Alder, R. W.; Moss, R. E.; Sessions, R. B. *J. Chem. Soc., Chem. Commun.* **1983**, 997. (b) Alder, R. W.; Orpen, A. G.; Sessions, R. B. *J. Chem. Soc., Chem. Commun.* **1983**, 999. (c) Schaefer, W. P.; Marsh, R. E. *J. Chem. Soc., Chem. Commun.* **1984**, 1555.

(6) Alder, R. W. *Tetrahedron* **1990**, *46*, 683.

(7) Alder, R. W.; Koetzle, T. F.; Orpen, A. C.; White, J. M. Personal communication to O. K. (unpublished results, neutron diffraction at 20 K; quoted in ref 6).

(8) From neutron diffraction at 20 K,[7] d_{sym} = 1.278(3) Å, N···N= 2.556(4) Å, i.e., a distance 0.030(5) Å longer than the corresponding N···N distance of 2.526(3) Å obtained by X-ray diffraction at room temperature. This *expansion* of the N···N distance on cooling, which is outside the 3σ error limits of the two N···N distances, appears to be real but external to the H-bond as such: it is more likely due to conformational changes with temperature in the compact ring system of the cation embedded in the crystal than to differences arising from the diffraction method, as it involves nitrogen atoms.

(9) Alder, R. W.; Moss, R. E.; Sessions, R. B. *J. Chem. Soc., Chem. Commun.* **1983**, 1000.

(10) (a) Scheiner, S.; Harding, L. B. *J. Am. Chem. Soc.* **1981**, *103*, 2169. (b) Scheiner, S. *J. Phys. Chem.* **1982**, *86*, 376.

(11) Cameron, E. M.; Louch, W. E.; Cameron, T. S.; Knop, O. *Z. Anorg. Allg. Chem.* **1998**, *624*, 1629.

(12) (a) Robertson, K. N. Doctoral thesis, Dalhousie University, 2001. (b) Robertson, K. N.; Kwiatkowski, W.; Cameron, T. S.; Knop, O. Manuscript in preparation.

(13) (a) Spackman, M. A.; Brown, A. S. *Ann. Repts. Prog. Chem., Phys. Chem.* **1994,** *91C*, 175. (b) Mallinson, P. R.; Woźniak, K.; Smith, G. T.; McCormack, K. L. *J. Am. Chem. Soc.* **1997**, *119*, 11502. (c) Espinosa, E.; Molins, E.; Lecomte, C. *Chem. Phys. Lett.* **1998**, *285*, 170. (d) Spackman, M. A. *Ann. Repts. Prog. Chem., Phys. Chem.* **1998**, *94C*, 177.

(14) Frisch, M. J.; Trucks, G. W.; Schlegel, H. B.; Gill, P. M. W.; Johnson, B. G.; Robb, M. A.; Cheeseman, J. R.; Keith, T. A.; Petersson, G. A.; Montgomery, J. A.; Raghavachari, K.; Al-Laham, M. A.; Zakrzewski, V. G.; Ortiz, J. V.; Foresman, J. B.; Cioslowski, J.; Stefanov, B. B.; Nanayakkara, A.; Challacombe, M.; Peng, C. Y.; Ayala, P. Y.; Chen, W.; Wong, M. W.; Andres, J. L.; Replogle, E. S.; Gomperts, R.; Martin, R. L.; Fox, D. J.; Binkley, J. S.; Defrees, D. J.; Baker, J.; Stewart, J. P.; Head-Gordon, M.; Gonzalez, C.; Pople, J. A. *Gaussian 94* (Revision B.2); Gaussian, Inc.: Pittsburgh, PA, 1995.

(15) Bader, R. F. W. AIMPAC series of programs. Department of Chemistry, McMaster University, Hamilton, ON, 1983.

(16) (a) Ramos, M.; Alkorta, I.; Elguero, J.; Golubev, N. S.; Denisov, G. S.; Benedict, H.; Limbach, H.-H. *J. Phys. Chem. A* **1997**, *101*, 9791. (b) Alkorta, I.; Elguero, J. *Struct. Chem.* **1999**, *10*, 157.

(17) O′Brien, S. E.; Popelier, P. L. A. *Can. J. Chem.* **1999**, *77*, 28.

(18) Hobza, P. *Ann. Repts. Prog. Chem., Phys. Chem.* **1997**, *93C*, 268.

(19) For other papers involving the $N_2H_7^+$ cation and related homoconjugated species, see ref 20.

(20) (a) Merlet, P.; Peyerimhoff, S. D.; Buenker, R. J. *J. Am. Chem. Soc.* **1972**, *94*, 8301. (b) Payzant, J. D.; Cunningham, A. J.; Kebarle, P. *Can. J. Chem.* **1973**, *51*, 3242. (c) Delpuech, J.-J.; Serratrice, G.; Strich, A.; Veillard, A. *Mol. Phys.* **1975**, *29*, 849. (d) Desmeules, P. J.; Allen, L. C. *J. Chem. Phys.* **1980**, *72*, 4731. (e) Glidewell, C.; Holden, H. D. *Acta Crystallogr.* **1982**, *B38*, 667. (f) Scheiner, S.; Szczęśniak, M. M.; Bigham, L. D. *Int. J. Quantum Chem.* **1983**, *23*, 739 (g) Del Bene, J. E.; Frisch, M. J.; Pople, J. A. *J. Phys. Chem.* **1985**, *89*, 3669. (h) Ikuta, S. *J. Chem. Phys.* **1987**, *87*, 1900. (i) Evleth, E. M.; Hamou-Tahra, Z. D.; Kassab, E. *J. Phys. Chem.* **1991**, *95*, 1213. (j) Bock, H.; Vaupel, T.; Näther, C.; Ruppert, K.; Havlas, Z. *Angew. Chem., Int. Ed. Engl.* **1992**, *31*, 299. (k) Del Bene, J. E.; Shavitt, I. *THEOCHEM* **1994**, *307*, 27. (l) Platts, J. A.; Laidig. K. E. *J. Phys. Chem.* **1995**, *99*, 6487. (m) Pudzianowski. A. T. *J. Chem. Phys.* **1995**, *102*, 8029. (n) Bock, H.; Vaupel, T.; Schödel, H. *J. Prakt. Chem.* **1997**, *339*, 26.

(21) (a) Berthold. H. J.; Preibsch, W.; Vonholdt, E. *Angew. Chem., Int. Ed. Engl.* **1988**, *27*, 1524. (b) Berthold, H. J.; Vonholdt, E.; Wartchow, R.; Vogt, T. *Z. Kristallogr.* **1992**, *200*, 225. (c) Berthold, H. J.; Vonholdt, E.; Wartchow, R.; Vogt, T. *Z. Kristallogr.* **1993**, *203*, 199. (d) Berthold, H. J. Personal communication to O.K.

(22) An N(sp^2)-hybridized species would be expected to fall between the ZC≡N−H and the $[Z_3N-H]^+$ donor species. Unfortunately, the prosymmetric type species tried, $(H_2C{=}N-H{\cdots}N{=}CH_2)^-$ and $[H_2C{=}N(H)-H{\cdots}N(H){=}CH_2]^+$, either did not optimize properly in any of the combinations HF/C_s, HF/C_{2h}, MP2/C_s, MP2/C_{2h} or when they did, the optimized configuration was not symmetric.

(23) Herzberg, G. *Molecular Spectra and Molecular Structure. Vol. 2. Infrared and Raman Spectra of Polyatomic Molecules;* Van Nostrand: New York, 1951.

(24) (a) Rozière, J.; Belin, C.; Lehmann, M. S. *J. Chem. Soc., Chem. Commun.* **1982**, 388. (b) Jones, D. J.; Brach, I.; Rozière, J. *J. Chem. Soc., Dalton Trans.* **1984,** 1795. (c) Teulon, P.; Delaplane, R. G.; Olovsson, I.; Rozière, J. *Acta Crystallogr.* **1985**, *C41*, 479.

(25) (a) Macdonald, A. L.; Speakman, J. C.; Hadži, D. *J. Chem. Soc., Perkin Trans 2*, **1972**, 825. (b) Currie, M.; Speakman, J. C.; Kanters, J. A.; Kroon, J. *J. Chem. Soc., Perkin Trans. 2* **1975**, 1549.

(26) This symmetry element is normally an inversion center, but other symmetry elements occasionally occur, usually in situations constrained by internal stereochemistry. The proton-spongelike cation in JACSAH (not included in Figure 4, but at the short end of the A−F range) is an example of a short, internally homoconjugated N−H−N bond with the H atom formally on a C_2 axis (XD, 196 K, D = 2.600(3) Å, d' = 1.30(5) Å, NHN = 169(2)°, $\Delta d'$ = 0.17 Å).[27]

(27) Alder, R. W.; Eastment, P.; Hext, N. M.; Moss, R. E.; Orpen, A. G.; White, J. M. *J. Chem. Soc., Chem. Commun.* **1988**, 1528.

(28) (a) Alkorta, I.; Barrios. J.; Rozas, I.; Elguero, J. *THEOCHEM* **2000,** *496*, 131. (b) Alkorta, I. Personal communication to R.J.B.

(29) (a) Csonka, G. I.; Nguyen, N. A.; Kolossvary, I. *J. Comput. Chem.* **1997**, *18*, 1534. (b) Hoffmann-Ostenhof, M.; Hoffmann-Ostenhof, T. *Phys. Rev.* **1977**, *A16*, 1782.

(30) (a) von Dreele, R. B.; Hanson, R. C. *Acta Crystallogr.* **1984**, *C40*, 1635. (b) Eckert, J.; Mills, R. L.; Satija, S. K. *J. Chem. Phys.* **1984**, *81*, 6034. (c) Loveday, J. S.; Nelmes, R. J.; Marshall, W. G.; Besson, J. M.; Klotz, S.; Hamel, G. *Phys. Rev. Lett.* **1996**, *76*, 74.

(31) (a) Howard, S. T.; Hursthouse, M. B.; Lehmann, C. W.; Poyner, E. A. *Acta Crystallogr.* **1995**, *B51*, 327. (b) Flensburg, C.; Larsen, S.; Stewart, R. F. *J. Phys. Chem.* **1995**, *99*, 10130. (c) Roversi, P.; Barzaghi, M.; Merati, F.; Destro, R. *Can. J. Chem.* **1996**, *74*, 1145. (d) Madsen, D.; Flensburg, C.; Larsen, S. *J. Phys. Chem. A* **1998**, *102*, 2177. (e) Flaig, R.; Koritsanszky, T.; Zobel, D.; Luger, P. *J. Am. Chem. Soc.* **1998**, *120*, 2227.

(32) Statistically acceptable single-exponential d,ρ_c regressions for O−H···O bonds, both for ab initio and experimental data, have been reported by Alkorta, I.; Elguero, J. *J. Phys. Chem. A.* **1999**, *103*, 272. Alternative models do not appear to have been tested in their investigation.